

AN AIRCRAFT WARNING BEACON

by

GEORGE ROBERT PICKERING

B.A.Sc., University of Toronto, 1976

A THESIS SUBMITTED IN PARTIAL FULFILLMENT OF  
THE REQUIREMENTS FOR THE DEGREE OF  
MASTER OF APPLIED SCIENCE

in

THE FACULTY OF GRADUATE STUDIES  
DEPARTMENT OF ELECTRICAL ENGINEERING

We accept this thesis as conforming  
to the required standard

THE UNIVERSITY OF BRITISH COLUMBIA

September, 1978

© George Robert Pickering, 1978

In presenting this thesis in partial fulfilment of the requirements for an advanced degree at the University of British Columbia, I agree that the Library shall make it freely available for reference and study.

I further agree that permission for extensive copying of this thesis for scholarly purposes may be granted by the Head of my Department or by his representatives. It is understood that copying or publication of this thesis for financial gain shall not be allowed without my written permission.

Department of Electrical Engineering

The University of British Columbia  
2075 Wesbrook Place  
Vancouver, Canada  
V6T 1W5

Date 29 September 1978

## Abstract

The Canadian Ministry of Transport recommends that powerline crossings on river valleys be marked by white flashing lights. In remote areas a power supply for these lights can be difficult to obtain.

A warning beacon system which uses the leakage current of semi-conductive glaze insulators to power a capacitive discharge flashtube is described. Consideration is given to the relevant characteristics of flashtubes and semiconductive glaze insulators.

Tests which have been conducted to confirm the viability of the system are described.

## TABLE OF CONTENTS

	Page
ABSTRACT	ii
TABLE OF CONTENTS	iii
LIST OF TABLES	iv
LIST OF ILLUSTRATIONS	v
ACKNOWLEDGEMENT	vi
I. INTRODUCTION	1
II. CAPACITIVE DISCHARGE FLASHTUBES	4
III. SEMICONDUCTIVE GLAZE INSULATORS	8
IV. TRANSFORMER - DESIGN CONSIDERATIONS	11
V. TRANSFORMER - MODEL	24
VI. BEACON POWER SUPPLY AND CONTROL CIRCUITS	32
6.1 Beacon Power Supply Circuit	32
6.2 Single Flashtube Control Circuit	32
6.3 Control Circuit for Three Flashtubes	37
VII. OBSERVED BEACON PERFORMANCE	41
VIII. CONCLUSIONS AND SUGGESTIONS FOR FURTHER WORK	44
APPENDIX A. STRAY CAPACITANCE IN THE TRANSFORMER	45
APPENDIX B. MAGNETIZING IMPEDANCE OF THE TRANSFORMER	50
APPENDIX C. CONTROL CIRCUIT WAVEFORMS	52
REFERENCES	56

## List of Tables

	Page
Table I. Power Available into a Battery Pack.	42
Table II. Battery Pack Charge Characteristic.	42

## List of Illustrations

Figure		Page
3.1	6-Unit Semicon String Model on a 230 kV Line	10
4.1	Bobbin for Primary Winding	14
4.2	Lamination Strain Calculation	16
4.3	Photograph of Transformer Core Assembly	18
4.4	Photograph of Transformer	19
4.5	Transformer Connection to 230 kV Line	21
4.6	Model for Transient Analysis of the Circuit of Figure 4.5	22
4.7	Transient Voltage at Node H in Figure 4.6	23
5.1	Stray Capacitance in the Transformer	26
5.2	Transformer Model	27
5.3	Power Delivered to a Resistive Load Using a Single Semicon String	28
5.4	Power Delivered to a Resistive Load Using Two Semicon Strings	30
5.5	Current Distribution for $R_L = 22 \text{ M}\Omega$	31
6.1.1	Beacon Power Supply	33
6.2.1	Single Flashtube Control Circuit	34
6.2.2	Waveforms of Control Circuit	36
6.3.1	Synchronizing Signal Generator for Three Single Flashtube Units	38
6.3.2	Three Lamp Control Circuit	40
7.1	Battery Pack Charge Characteristic	43
A.1	Stray Capacitances	46
B.1	Transformer Magnetizing Impedance	51
C.1	Discharge Capacitor Charging Circuit	53

## ACKNOWLEDGEMENT

I wish to thank Dr. A.D. Moore for his assistance throughout the course of my stay at the University of British Columbia.

Valuable advice on the construction of the transformer was provided by Mr. H. Burgess of the British Columbia Transformer Company Limited. Mr. R.A. Briggs of Cor-Mag Company supplied the material used in the transformer core.

Thanks are also due to Mr. A. Reed of the British Columbia Hydro and Power Authority for his advice and his assistance in arranging for testing of the prototype.

The technical staff of the University of British Columbia deserves a great deal of credit. In particular I would like to thank Mr. D. Daines and Mr. D. Fletcher for constructing the prototype, and Mr. A. MacKenzie for his assistance in testing the prototype and in dealing with bureaucratic red tape.

The manuscript was typed by Mrs. S.Y. Hoy.

I would also like to thank Dr. H.W. Dommel for reading the thesis, and for the use of his computer program.

This research was supported in part by NRC grant A-3357, and by a grant from the British Columbia Hydro and Power Authority.

## I. INTRODUCTION

It is common practice for small aircraft to use river valleys as navigation aids, especially during periods of low visibility. The hazard introduced by power lines crossing the valleys is well recognized. At present these obstructions are marked, in most cases, by painting the towers on each side of the valley, and by suspending reflective spheres from the catenary. To increase the visibility of the lines the Canadian Ministry of Transport [1] recommends that high intensity white flashing lights be mounted on the towers at crossings. Three lights, one located at the top of the tower, one at the level of the lowest point of the catenary, and one midway between, serve to provide an indication of the position of the power cables. As stated in the Ministry's recommendations [1]

The white lights shall flash sequentially; first the middle light, then the top light and last, the bottom light. The off interval between the top light and the bottom light shall be twice as long as the interval between the middle light and the top light. Interval between the end of one sequence and the beginning of the next shall be about 10 times the interval between the middle and top light. Each light unit of the system shall flash at a rate of 40 to 60 per minute; 60 per minute preferable.

One of the major problems encountered when attempting to develop such a warning beacon system is providing a source of power for the lights. Where a low voltage distribution network is nearby this problem does not arise, but many river crossings exist in remote areas where no such network is available. Several methods have been developed to solve this problem, all consisting of a way of obtaining power from the high voltage line itself. The amount of power required depends upon the type of beacon desired.



A typical unit approved by the Federal Aviation Authority of the United States consumes in excess of 200 W. The xenon flashtube units used on aircraft operate at approximately 25 W.

The current flowing in a power line will induce a current in any nearby conductive loop. This principle has been used by H.J. Dana [2] to provide power for a mid-catenary neon warning light. In this system an iron core is clamped around the conductor. A many-turn secondary on the core is connected to a neon tube, which produces a steady red light. It would appear that this technique could also be used to power a flashing light system. However, since the current in the line fluctuates over a wide range, the amount of power available is not well defined.

L'Institut de recherche de l'Hydro-Quebec (IREQ) has developed a system which obtains power from the high voltage line using electrostatic coupling between the overhead ground wire and the line [3,4]. Overhead ground wires are strung above the power lines to provide lightning protection. Capacitance exists between the overhead ground wire and the lines, the value of which depends upon the physical dimensions involved and the atmospheric conditions. For the line configuration studied by IREQ, this capacitance is 6.5 pF/m. To collect the energy coupled to the overhead ground wire by this capacitance, the wire is electrically isolated from the towers, and connected to a step-down transformer. IREQ has obtained 5 kW/km from a 735 kV line, and has used a single span to power a beacon containing two 100 W incandescent lamps. The amount of power available from a capacitive system depends upon the line voltage rather than the current, and should thus fluctuate less than the power obtained by inductive coupling.

Overhead ground wires are only used in very few places on the power lines of the British Columbia Hydro and Power Authority, so that the use of a system of the type developed by IREQ would require considerable modification of the existing lines. The system described in this thesis, which was developed in cooperation with the British Columbia Hydro and Power Authority, uses the leakage current of semiconductive glaze insulators to supply power for a xenon flashtube warning beacon. This leakage current depends upon the line voltage and the atmospheric conditions. Because the characteristics of the insulators and flashtubes have a significant influence on the design of the warning beacon system, they will be considered before the system itself is described.

## II. CAPACITIVE DISCHARGE FLASHTUBES

A flashing light can be obtained from a flashtube, or by switching an incandescent lamp on and off. Capacitive discharge flashtubes are superior to flashed incandescent lamps for use as warning beacons due to their higher luminous efficacy, higher effective intensity, and longer life.

Luminous efficacy is the total visible luminous flux output (in lumens) divided by the total power input (in watts) [5]. Xenon flashtubes produce between 10 and 50 lumens per watt, with a typical value of 35 lm/W. Incandescent lamps normally produce approximately 10 lm/W.

At low levels of illumination, the effective intensity of a flashing light is given by [6]

$$I_E = \frac{\int_{t_1}^{t_2} I(t) dt}{a + (t_2 - t_1)}$$

where  $I(t)$  is the light intensity at time  $t$ , (lm),  $a$  is the Blondel-Rey constant normally taken to be 0.2 seconds,  $t_1$ ,  $t_2$  (seconds) are chosen so as to maximize  $I_E$ .

For a capacitive discharge lamp,  $t_1$  and  $t_2$  are the beginning and end of the discharge and  $(t_2 - t_1)$  is much less than 0.2 s. Thus, for such a lamp

$$I_E \approx 5 \int_{t_1}^{t_2} I(t) dt$$

A flashed incandescent lamp usually has a duration  $(t_2 - t_1)$  greater than 0.2s. Consequently, given a discharge lamp and a flashed incandescent lamp with the same value of integrated intensity, the discharge lamp will be more effective.

Incandescent lamps have a short life which is reduced considerably by the continuous heating and cooling of the element resulting from switching the unit on and off.

Flashtubes are subject to two main failure mechanisms. Cracking or crazing of the wall of the tube can occur if the current density of the arc is too high. Blackening of the tube caused by sputtering of the cathode material due to bombardment by high velocity atoms of the fill gas will also occur. Both of these failure mechanisms depend upon the applied energy per flash; it has been found that reducing the energy by half results in a ten-fold increase in the life of the tube. Lifetimes of  $10^8$  flashes are possible, so that a warning beacon operating at a rate of one flash per second could last longer than three years.

Inert gases are normally used in flashtubes, since their outermost atomic orbits are full of electrons, making them readily excitable. Of the inert gases, xenon is most often used because it has the largest collision cross-section and the lowest excitation and ionization potentials, as well as an output spectral distribution which most closely approximates daylight.

There are three main criteria to be considered when applying a flashtube. The first two, flash duration and anode voltage are interrelated. Flash durations of less than 10  $\mu$ s are possible. However, to obtain significant light output from such a flash, a high anode voltage (perhaps 15 kV) would be required, resulting in a high current density and attendant problems in tube design. In addition, a shift in the spectral distribution of the light output towards ultraviolet would occur. For consistent operation at low anode voltages (i.e. about 200 V), low fill pressure is necessary.

This results in low energy-handling capability, low luminous efficacy, and a spectral shift towards infrared. Practical figures for warning beacon applications are anode voltage between 300 V and 2 kV and flash duration of 100  $\mu$ s to 10 ms.

The third criterion is triggering method. Flashtubes are operated with anode voltages well below self-ionization voltage levels, which are typically greater than 500 V per inch of arc length. Three methods are commonly used for initiating the arc: external shunt triggering, internal shunt triggering, and series injection triggering. External shunt triggering consists of applying a high voltage (greater than 4 kV) pulse to a wire or conductive film on the outside of the flashtube. This ionizes some of the fill gas atoms, initiating the arc. The pulse is usually generated by discharging a small capacitor through the primary of a pulse transformer, the secondary of which is connected to the trigger terminal of the tube. Internal shunt triggering differs only in that the trigger pulse is applied to a third electrode inside the flashtube. This allows a lower voltage pulse to be used, but increases the complexity of the tube.

In series injection triggering, the secondary of the trigger transformer is placed in series with the anode of the flashtube. The trigger pulse raises the anode voltage above the self-ionization voltage of the tube. The other circuit components must withstand the trigger voltage, and the pulse transformer secondary must be capable of carrying the discharge current. Series injection triggering does not apply high voltage to the outside of the tube as in external shunt triggering, and thus possible blackening of the glass is avoided.

The system described herein uses external shunt triggering and an anode voltage of approximately 350 V. This allows the use of readily available, reasonably priced flashtubes.

### III. SEMICONDUCTIVE GLAZE INSULATORS

When a contaminated insulator becomes wet, its breakdown voltage is greatly reduced. It has been found that the surface may be kept dry if it is maintained at a temperature a few degrees above ambient. This can be done by coating the insulator with a conductive glaze. The current flowing through the glaze provides the desired heating effect. Modern insulators of this type use an antimony-doped stannic oxide glaze, and are referred to as "semiconductive glaze insulators" (or "semicons").

One such insulator has been developed by the Canadian Porcelain Company Limited in cooperation with the Hydro-Electric Power Commission of Ontario [7]. It has a deep bell shape which shields much of the surface from direct wetting, enabling the drying effect of the semiconductive glaze to be effective even during heavy rain. This insulator has a 60 Hz withstand voltage of 30 kV per unit when heavily contaminated, which is approximately double that of a conventional glaze insulator. The shorter strings which may thus be used allow the design of more compact transmission lines, as well as the upgrading of existing lines to higher voltage while maintaining adequate ground clearance.

Standard glaze insulators have a 60 Hz impedance of approximately  $85 \text{ M}\Omega$ , which is due to a pin to cap capacitance of about 30 pF. A bell-shaped, semiconductive glaze insulator has, in addition to pin to cap capacitance, a resistive path along its surface, and capacitance between the inside and outside surfaces. This distributed R-C network may be represented approximately by a resistor and a capacitor in parallel.

Since the resistance of the semiconductive glaze has a negative temperature coefficient, low resistance insulators are prone to thermal runaway. If the resistance of the glaze is too high, the desired heating effect is lost. These considerations limit useful insulators to d.c. resistances between 20 and 100 M $\Omega$ . For this range of d.c. resistances, the parallel resistance and capacitance of the lumped model lie between 13 M $\Omega$  and 60 M $\Omega$ , and 110 pF and 80 pF respectively.

When the insulators are connected together to form a string, capacitance between units and capacitance from each unit to ground must be considered. By measuring the voltage distribution in a string of insulators using a calibrated sphere gap, Rau [8] has been able to develop the model for a six unit string shown in Figure 3.1.  $R_p$  and  $C_p$  represent the semicon insulators. The currents shown were obtained by computer analysis using a source voltage of 132.8 kV (230 kV line to line), and  $R_p = 35$  M $\Omega$ ,  $C_p = 80$  pF.



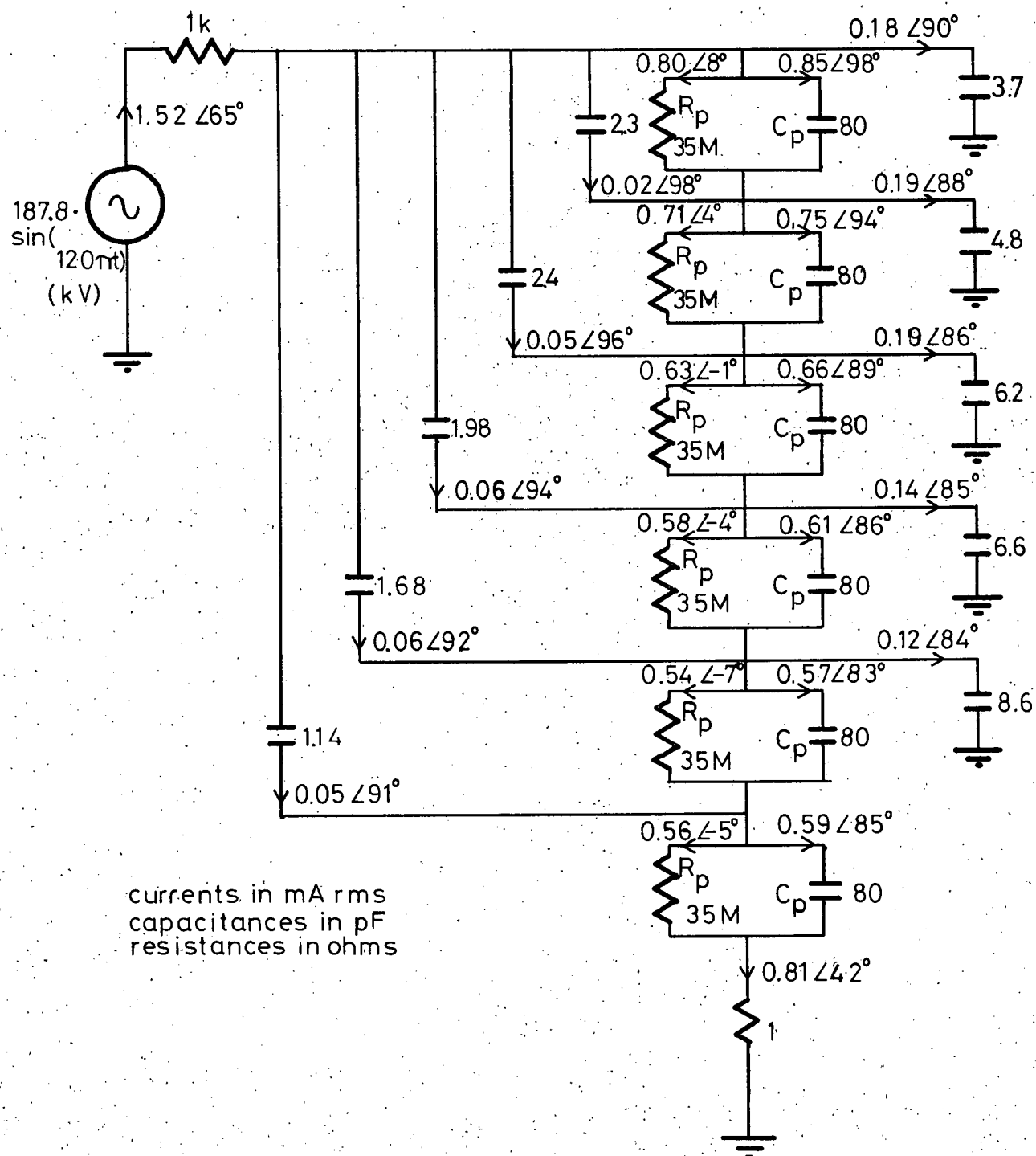


### Figure 3.1-Model For a 6-unit Semicon String On a 230kV Line

#### IV. TRANSFORMER - DESIGN CONSIDERATIONS

In order to use the leakage current of a semiconductive glaze insulator string to power a warning beacon, some means of collecting the current and transforming it to a usable level is required. The low voltage end of the semicon string is normally connected to the tower, allowing the leakage current to flow to ground. Collecting the current may be accomplished by inserting a number of standard glaze insulators between the semicon string and the tower, and tapping off at the low voltage end of the semicons. The number of standard glaze insulators required is determined by the maximum expected voltage at the tap-off point.

A transformer was designed to convert the leakage current to a higher level at a lower voltage. 20 kV was chosen as the maximum primary voltage. This is the normal operating voltage across each semiconductive glaze insulator, and therefore produces less than a twenty per cent disturbance in the voltage distribution across a six unit string. In addition, it is high enough to allow a useful amount of power to be obtained, but not so high as to unduly complicate the transformer design. For this primary voltage, two standard glaze insulators are required between the semicon string and the tower.

Grain-oriented silicon steel (type M-4) was used to make the core of the transformer. This material has high permeability at high flux density in the rolling direction, as well as low loss. It has a thickness of 0.011 inches and is coated with an insulating layer of magnesium silicate, thus allowing many laminations to be used in a core without giving rise to eddy current problems.

For sinusoidal excitation, the voltage-flux density relationship for a coil is

$$|V_m| = NA \omega B_m$$

where  $V_m$  is the peak value of the applied voltage (volts)

$N$  is the number of turns

$A$  is the cross-sectional area of the flux path ( $m^2$ )

$\omega$  is the angular frequency of the applied voltage (radians/s)

$B_m$  is the peak flux density (Tesla)

M-4 type silicon steel enters saturation at  $B_m \approx 1.7$  Tesla. At this flux density level, loss is approximately 0.77 W per pound of steel. For a coil with a core of magnetic material,  $A = \alpha A_1$  where  $A_1$  is the cross-sectional area of the core and  $\alpha$  is the "stacking factor" which accounts for insulation and air space between the laminations of the core. For M-4 type steel  $\alpha = 0.966$  when the laminations are subjected to a pressure of 10 psi. Machine-wound toroids should approach this pressure, and since this was the type of core considered for the transformer, a value of  $\alpha = 0.95$  was used in the calculations. Because the iron loss of the transformer is directly proportional to the amount of steel used, it is desirable to minimize  $A_1$ . However, if  $A_1$  is too small, an impractical number of turns ( $N$ ) would be required. With a cross-section of one square inch, the number of primary turns should be

$$N = \frac{V_m}{\alpha A_1 \omega B_m} = 72 \times 10^3 \text{ turns.}$$

This value of  $N$  was thought to be reasonable.

The primary was wound with 32 AWG magnet wire, since this was about the smallest size that could be handled conveniently using the available coil winding equipment. The insulation on this wire is rated to withstand 800 V. In order to allow for imperfect winding, flows in the insulation, and possible overvoltages, an operating voltage of 50 V between adjacent windings (25 V per layer) was chosen. To obtain this value, the primary was wound on six two-segment bobbins. At a primary voltage of 20 kV, the voltage per turn is 0.39V. Thus to obtain 25V per layer, the layers must be composed of about 63 turns. Each of the 12 segments of the coil must have 6000 turns, so that approximately 95 layers are required. On the basis that 32 AWG wire could be wound 103 turns per inch, bobbins of the dimensions shown in Figure 4.1 were constructed. A slot beneath the central flange was provided so that the two segments of the coil could be joined at the inside of the winding. The two segments were then wound in opposite directions, thus giving two coils connected in series without the insulation problems inherent in running a lead from the inside layer of the winding to the outside.

A toroidal shape for the core was chosen for several reasons. In order to take advantage of the high permeability of M-4 type steel, the magnetic flux must be aligned with the rolling direction of the material, and the reluctance of any air gaps must be minimal. A toroid wound from a continuous strip of steel fulfils both of these requirements.

The lower limit on the size of the core is fixed by the necessity of fitting the windings onto it. A toroid provides the greatest enclosed area for a given amount of material, and one with an inside diameter of seven inches was found to be large enough for the coils used. Since the density of silicon steel is  $7.65 \text{ gm/cm}^3$ , the weight of the core is 6.6 pounds,

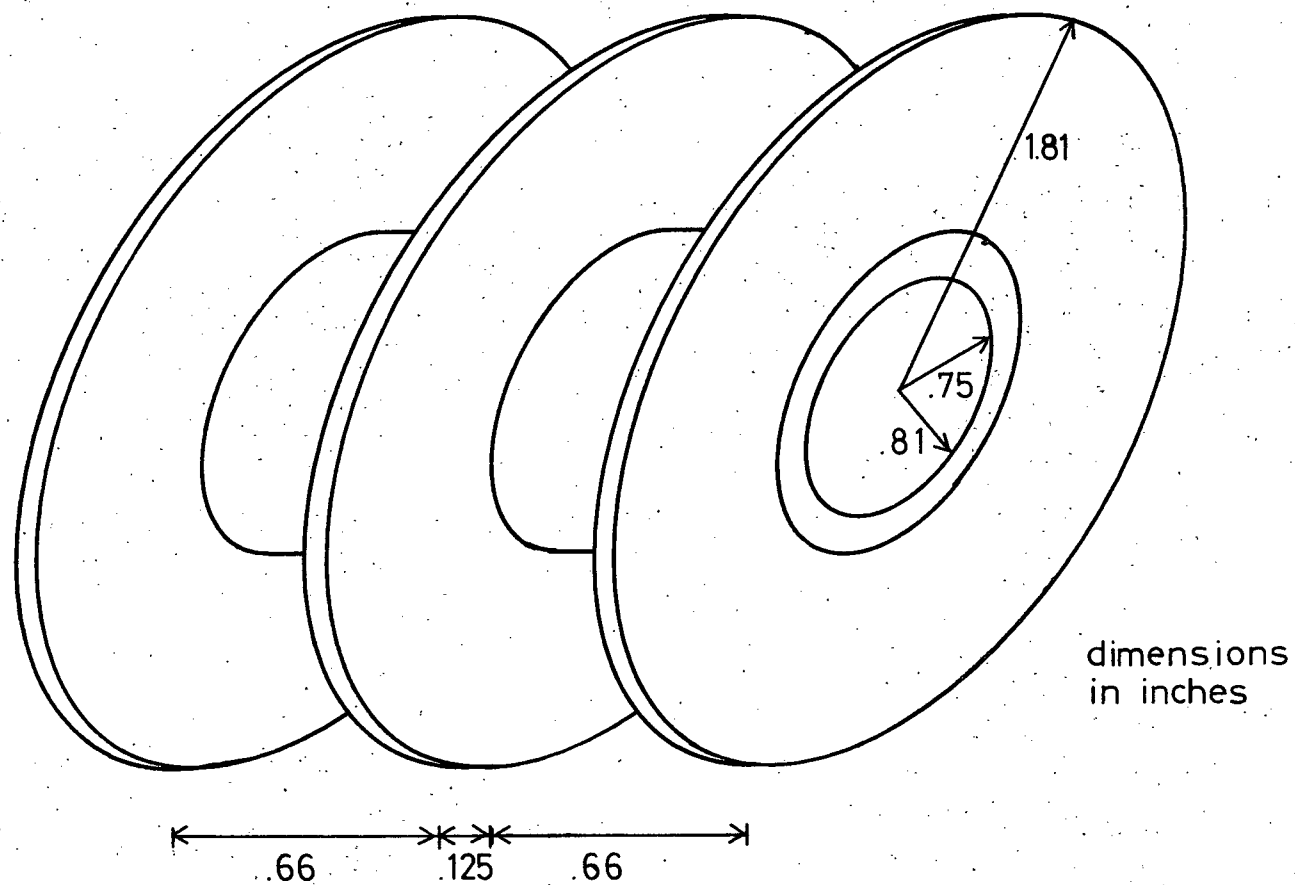


Figure 4.1-Bobbin For Primary Winding

and thus a loss of 5.1 Watts at a flux density of 1.7 Tesla was expected.

After any cold working of grain-oriented material, a stress-relief anneal is required to restore its magnetic properties. Since the temperatures used in the annealing process would destroy both the coil forms and wire insulation, it is important that the insertion of the core into the coils involve no cold working. The stress produced in the material by winding it into a seven inch inside diameter toroid may be calculated as follows. Consider a small section of the inside layer and let

$r_1$  = radius to inside of layer

$r_2$  = radius to outside of layer

$$r_n = \frac{r_1 + r_2}{2}$$

$\theta$  = the angle subtended by the section

(see Figure 4.2). Before winding, the length of the segment was  $r_n \theta$ . After winding, the outside of the segment has a length of  $r_2 \theta$ .

$$\begin{aligned} \text{Strain} &= \frac{\text{change in length}}{\text{original length}} \\ &= \frac{r_2 \theta - r_n \theta}{r_n \theta} \\ &= \frac{r_2 - r_1}{r_2 + r_1} \end{aligned}$$

$$r_1 = 3.5 \text{ inches}$$

$$r_2 = 3.511 \text{ inches}$$

$$\text{Therefore strain} = 1.569 \times 10^{-3}$$

The modulus of elasticity for M-4 type silicon steel in the rolling direction is  $19 \times 10^6$  psi. Therefore the stress is  $31.5 \times 10^3$  psi. Since the yield strength is  $48 \times 10^3$  psi, this stress is within the elastic limits

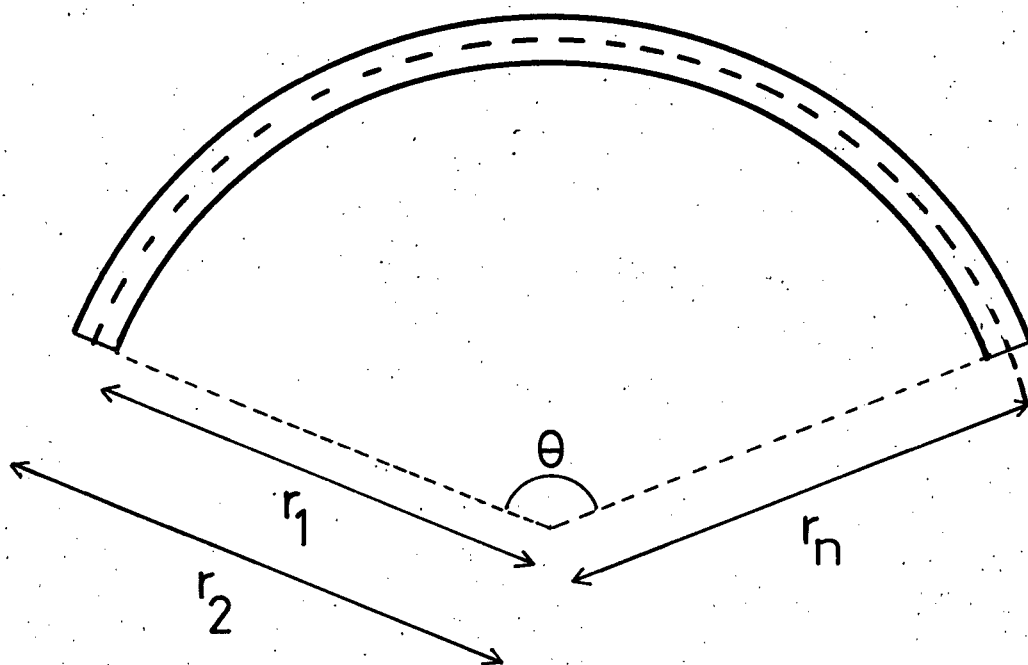


Figure 4.2 - Lamination Strain Calculation

of the material, and consequently no stress-relief anneal should be required after winding.

A toroid of 7 inch inside diameter and 91 layers (i.e. 1 inch of magnetic material) was wound from a continuous strip of 1 inch wide M-4 type steel supplied by the Cor-Mag Company of Burlington, Ontario. After the toroid had been annealed, the primary coil forms were mounted in a circle, and the core was wound through the forms.

Two secondary windings were added to the transformer after the core had been wound through the primary. These were wound using 24 AWG magnet wire. The first has 1018 turns providing a peak voltage of 400V, which can be used to charge either the discharge capacitor of the warning beacon or a high voltage battery pack. The second winding has taps at 76, 89, 102, 115, 127, 140 and 153 turns, and is used to tune the magnetizing impedance of the transformer to approximately unity power factor. Figure 4.3 is a photograph of the completed core assembly.

To provide sufficient dielectric strength between the various parts of the transformer, the core and coils are immersed in oil. For this purpose a steel can surmounted by a standard 35 kV bushing was constructed. A terminal block mounted above the level of the oil allows connections to the low-voltage windings to be made. The core is mounted in the can using "U"-shaped aluminum standoffs lined with plexiglass (these can be seen in Figure 4.3). The plexiglass provides electrical isolation between the core and the can, thus reducing the effect of stray capacitance between the primary and the core. Figure 4.4 is a photograph of the completed transformer.



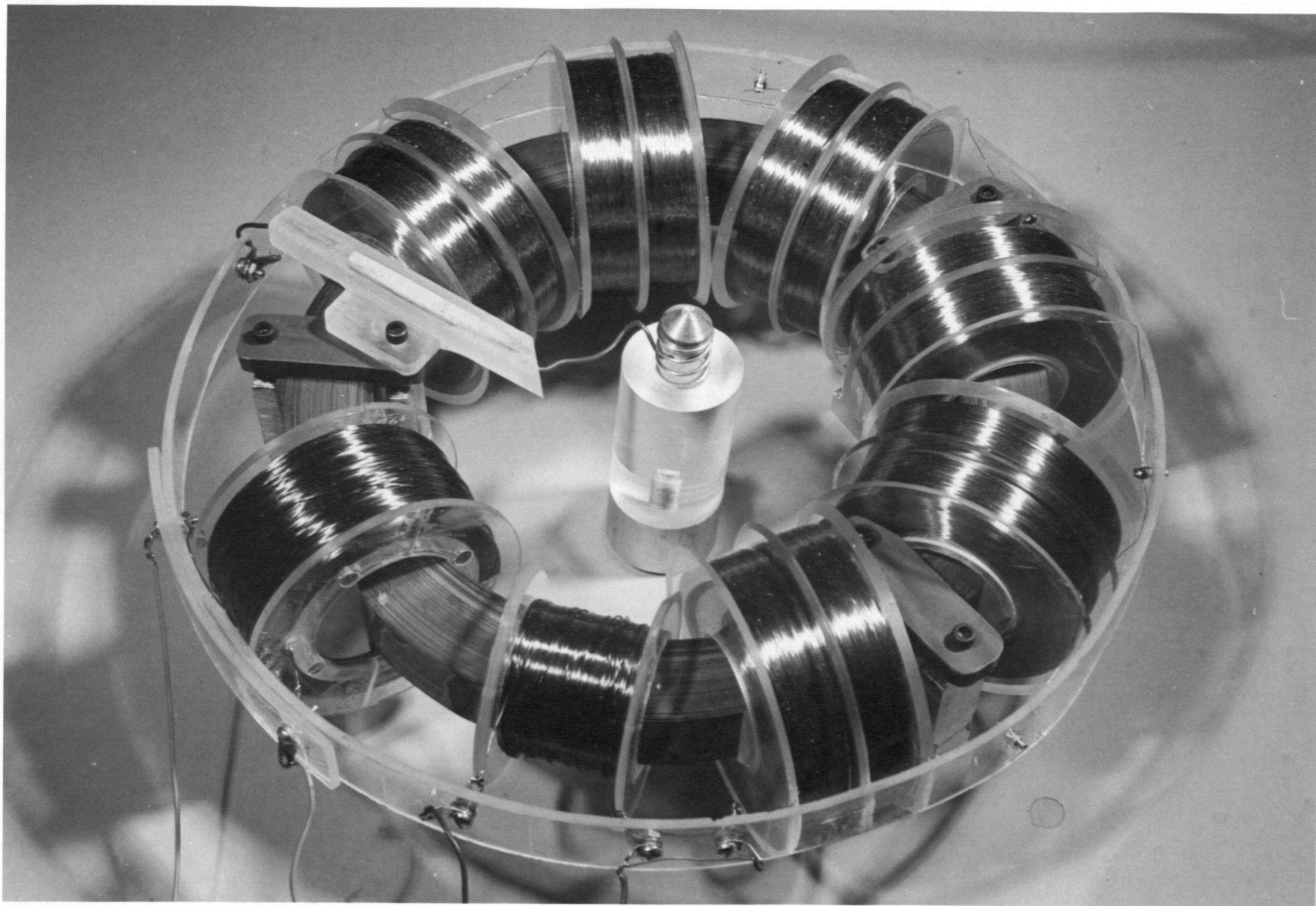


Figure 4.3 - Photograph of Transformer Core Assembly.

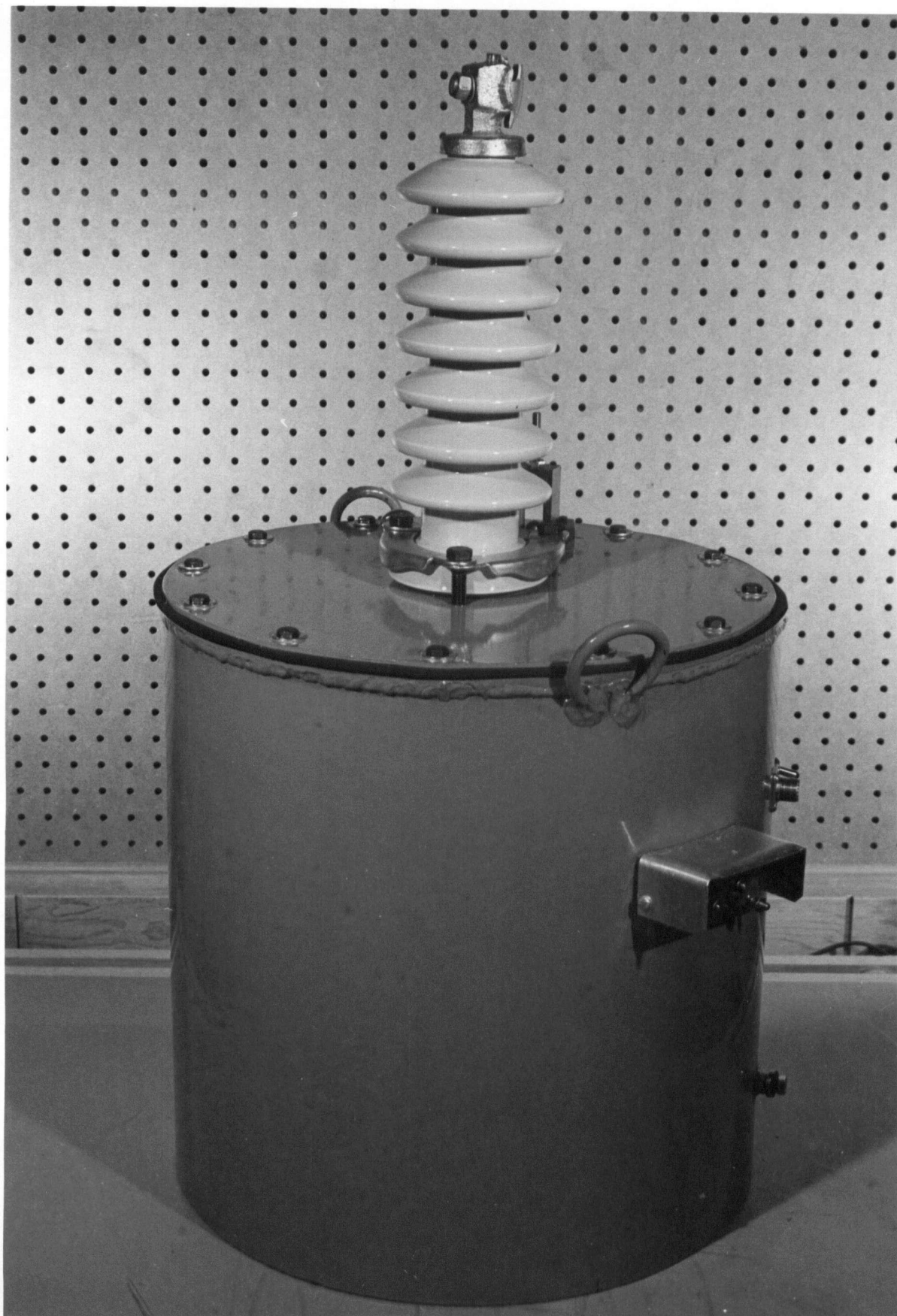


Figure 4.4 - Photograph of Transformer.

Figure 4.5 shows the manner in which the transformer is connected to the line. Two strings of semiconductive glaze insulators connected in parallel are shown since this is the configuration used in the final prototype. Because the capacitance of standard glaze insulators is much less than that of semiconductive glaze insulators, the transformer may be subjected to transient high voltage levels if the line is switched on at a peak of the voltage waveform. The behaviour of the transformer under these conditions is difficult to predict, but its interwinding capacitance should reduce the level of the transient. Thus a worst case value of the over-voltage can be obtained by representing the transformer as an open circuit under transient conditions. The resulting circuit model is shown in Figure 4.6. The voltage waveform at node H which results when the line is switched on at peak voltage was obtained by computer analysis and is shown in Figure 4.7. The peak level of 77 kV is about 3 times the normal operating voltage, indicating that some sort of protection for the transformer is required. A spark gap is mounted on the transformer can to provide this protection.

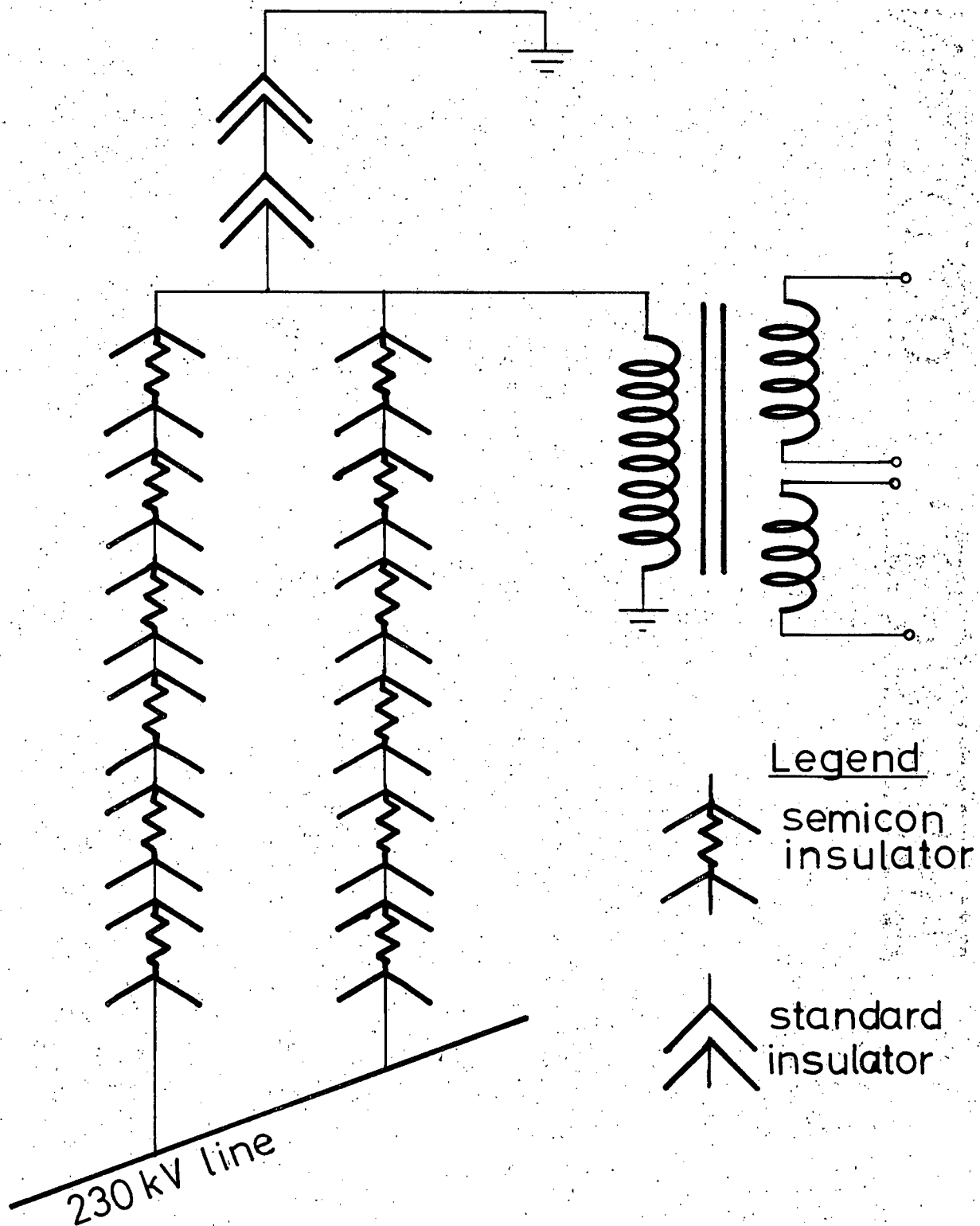


Figure 4.5- Transformer Connection To 230 kV Line

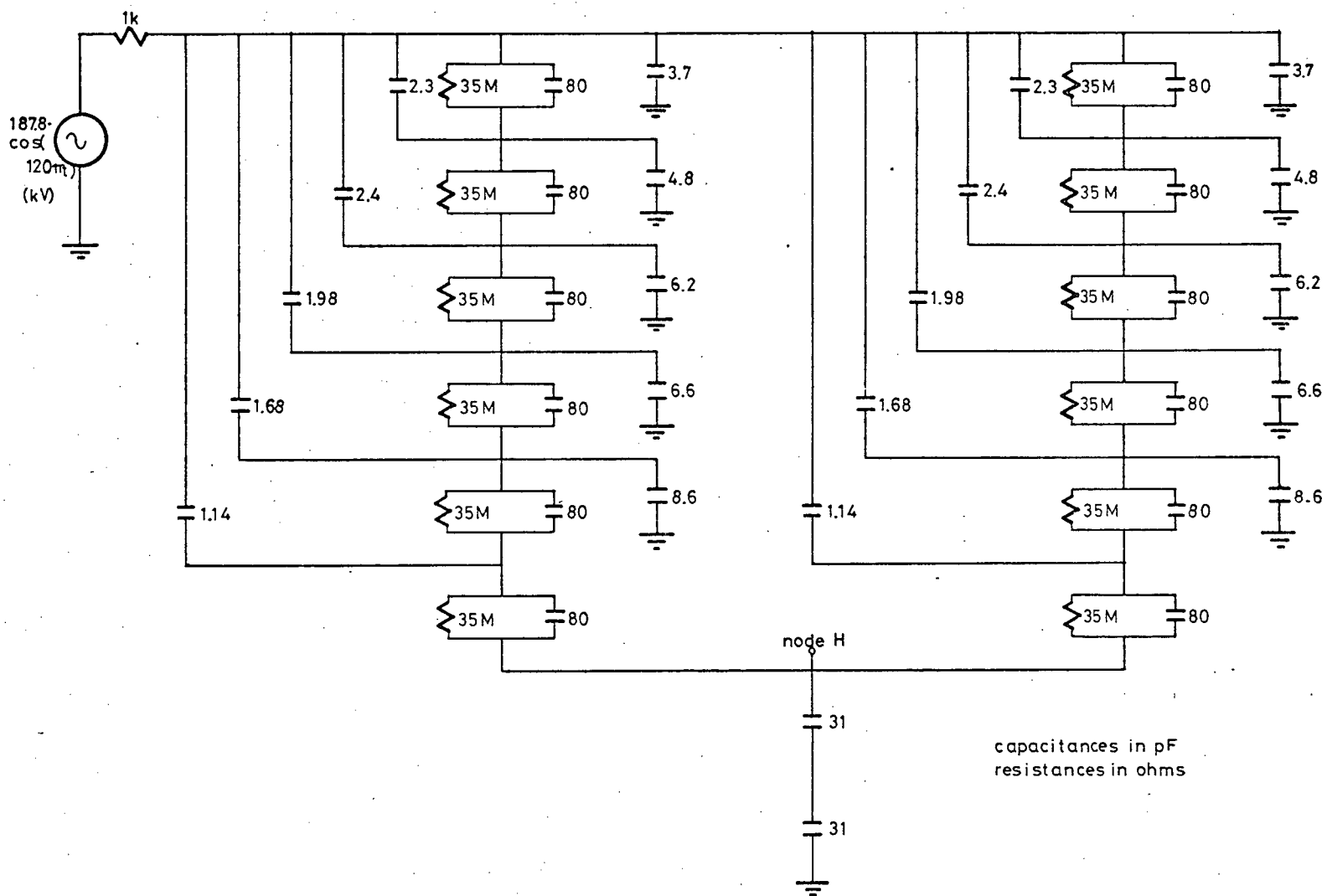


Figure 4.6—Model For Transient Analysis of the Circuit of Figure 4.5

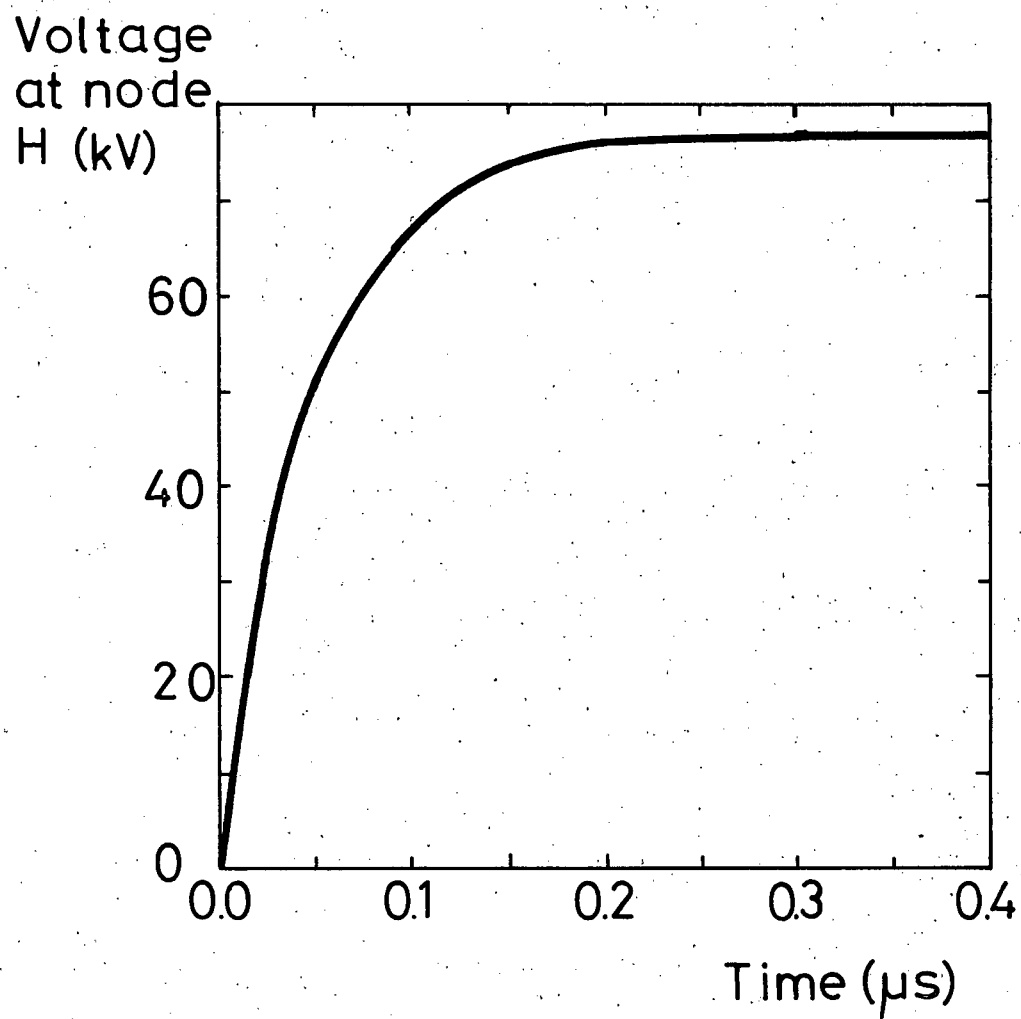


Figure 4.7 – Transient Voltage at Node H in Figure 4.6

## V. TRANSFORMER - MODEL

In order to predict the performance of the transformer, a series of measurements were made to determine a circuit model for it. The model is applicable in the steady state when the voltages are below the saturation level of the transformer.

Standard short circuit tests gave values for the total copper loss and leakage inductance. The leakage inductance was assumed to be evenly divided between the two windings, while the copper loss was split in proportion to their d.c. resistances.

Because of the low core loss and high magnetizing inductance, stray capacitance has a significant influence on the open circuit input impedance of the transformer. In addition to the interwinding capacitance, capacitances between the primary and core, primary and can, and core and can must be considered. Under the assumption of perfect coupling and negligible core loss, it can be shown (Appendix A) that the effective steady state capacitance is

$$C_{\text{eff}} = C_t + \frac{C_0 + C_2}{3} - \frac{C_0}{4(1 + \frac{C_1}{C_0})}$$

where  $C_t$  is the total interwinding capacitance

$C_0$  is the capacitance from primary to core

$C_1$  is the capacitance from core to can

$C_2$  is the capacitance from primary to can

Since the secondaries operate at a potential close to ground, the capacitance between the core and the secondaries is included in  $C_1$ . By measuring

the interwinding capacitance of a two-segment coil like those used to form the primary of the transformer,  $C_t$  was found to be 42 pF. The other stray capacitances were measured with a capacitance meter. The results are shown in Figure 5.1. Using these values ( $C_0 = 134$  pF,  $C_1 = 109$  pF,  $C_2 = 98$  pF) gives  $C_{eff} = 101$  pF.

Standard open circuit tests were used to determine the magnetizing impedance. It can be shown (Appendix B) that

$$L_m = \frac{2\omega^2 C_{eff} R_m Z^2 \pm \sqrt{[4\omega^4 C_{eff}^2 R_m^2 Z^4 - 4Z^2 R_m^2 (\omega^2 Z^2 - \omega^2 R_m^2 + \omega^4 Z^2 C_{eff}^2 R_m^2)]}}{2 [\omega^2 Z^2 - \omega^2 R_m^2 + \omega^4 Z^2 C_{eff}^2 R_m^2]}$$

where  $L_m$  is the magnetizing inductance (H)

$R_m$  is the real part of the magnetizing impedance ( $\Omega$ )

$Z$  is the magnitude of the magnetizing impedance ( $\Omega$ )

$\omega$  is the angular frequency of the applied voltage (rad./s)

$$R_m = \frac{V_{in}^2}{P_{in}}$$

$$Z = \frac{V_{in}}{I_{in}}$$

where  $V_{in}$  is the applied voltage

$I_{in}$  is the input current

$P_{in}$  is the input power

Figure 5.2 shows the complete transformer model. This model was used in conjunction with the insulator string model of Figure 3.1 to predict the power that could be obtained from a 230 kV line into a resistive load ( $R_L$ ).

Figure 5.3 is a graph of the power output versus load resistance obtained by computer analysis. The maximum value of approximately 5.8 W is



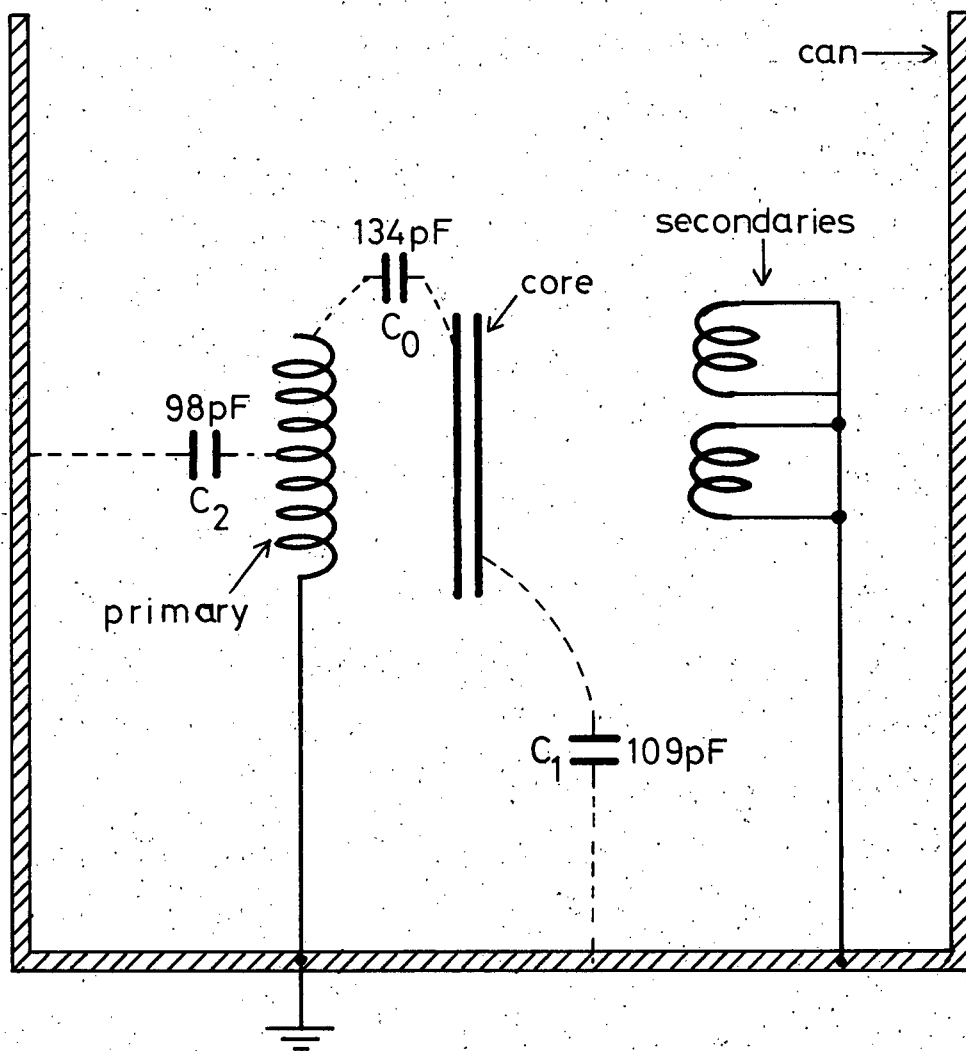


Figure 5.1-Stray Capacitance in the Transformer

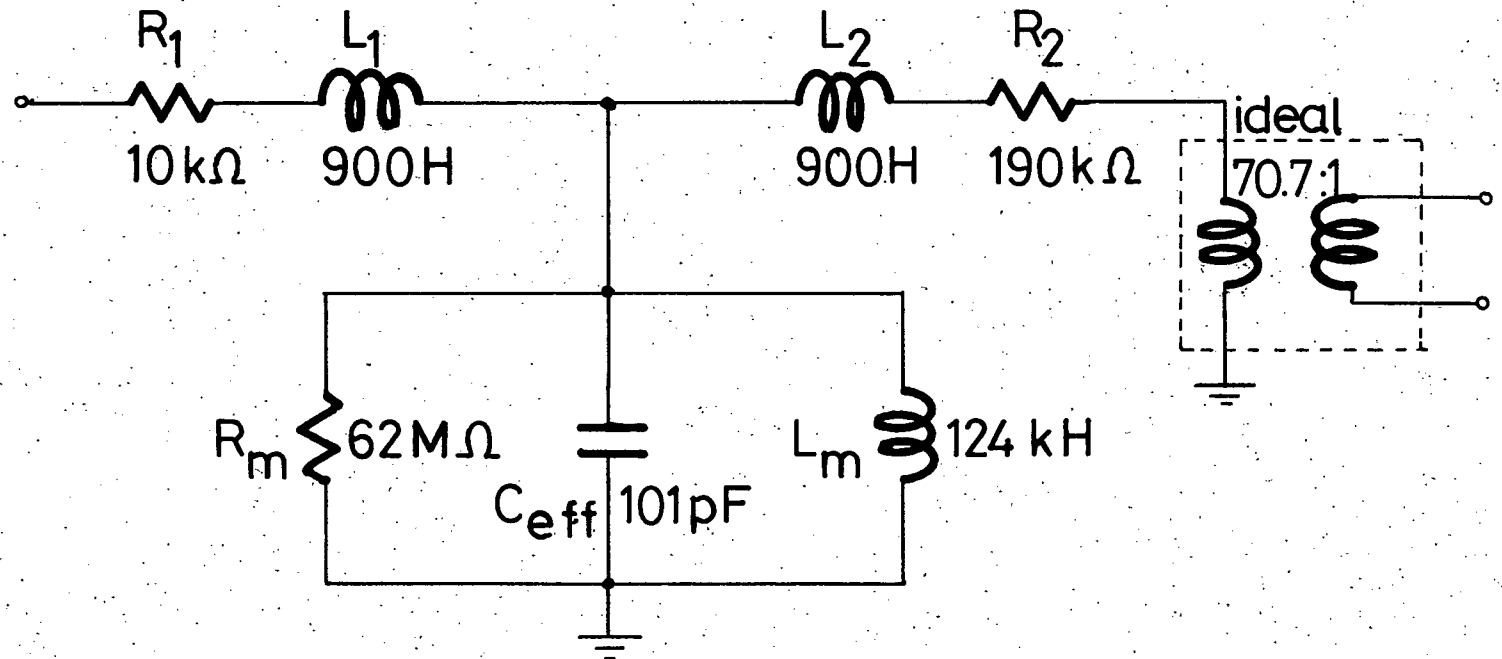


Figure 5.2 – Transformer Model

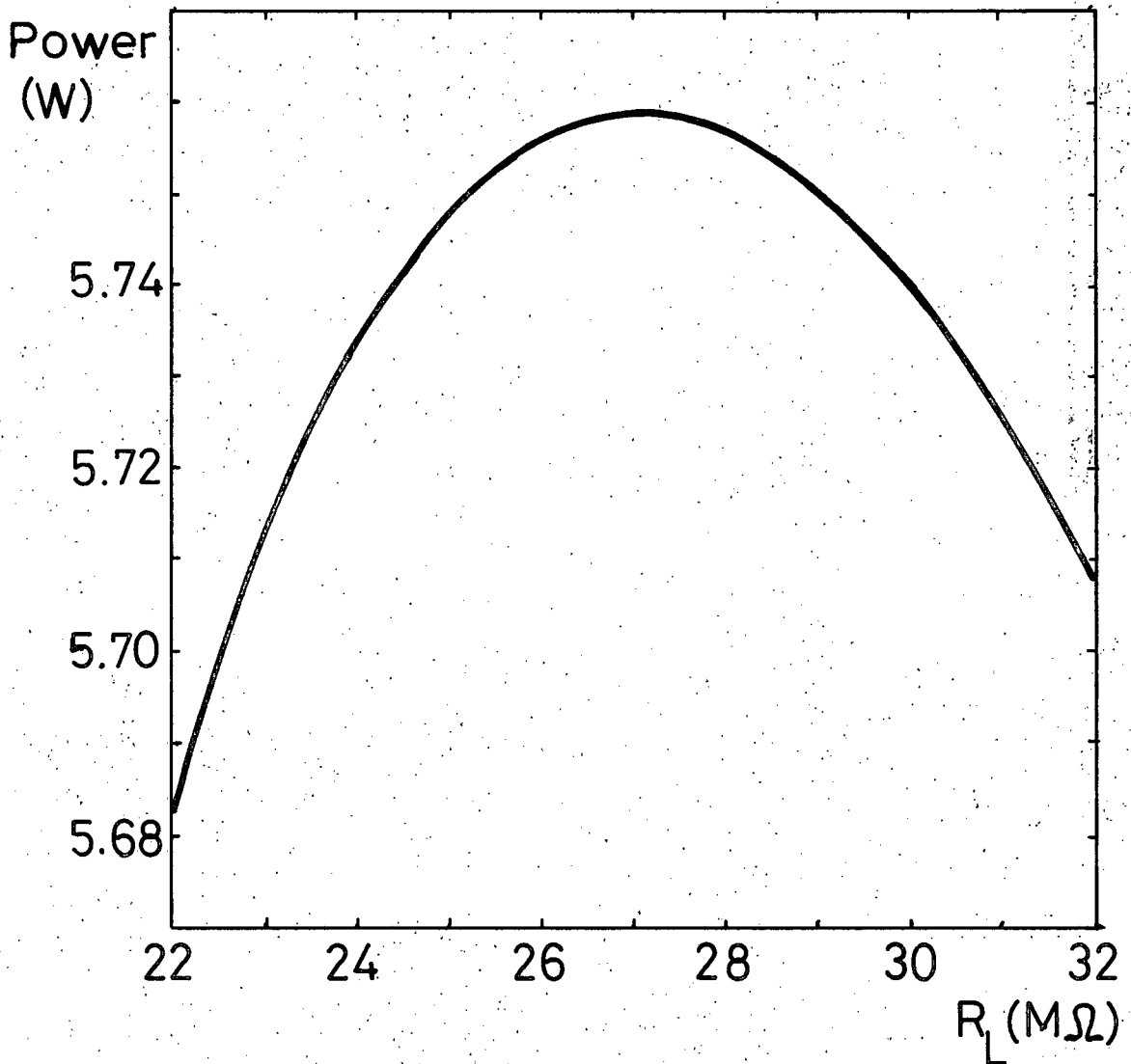


Figure 5.3 – Power Delivered To a Resistive Load Using a Single Semicon String

insufficient to supply a warning beacon. To obtain more power, two semi-conductive glaze insulator strings may be connected in parallel between the line and the transformer primary. Figure 5.4 shows the power obtained in this case, and Figure 5.5 shows the current distribution for  $R_L = 22 \text{ M}\Omega$ . The available power of approximately 18.5 W is sufficient to run a beacon of the type used on aircraft.

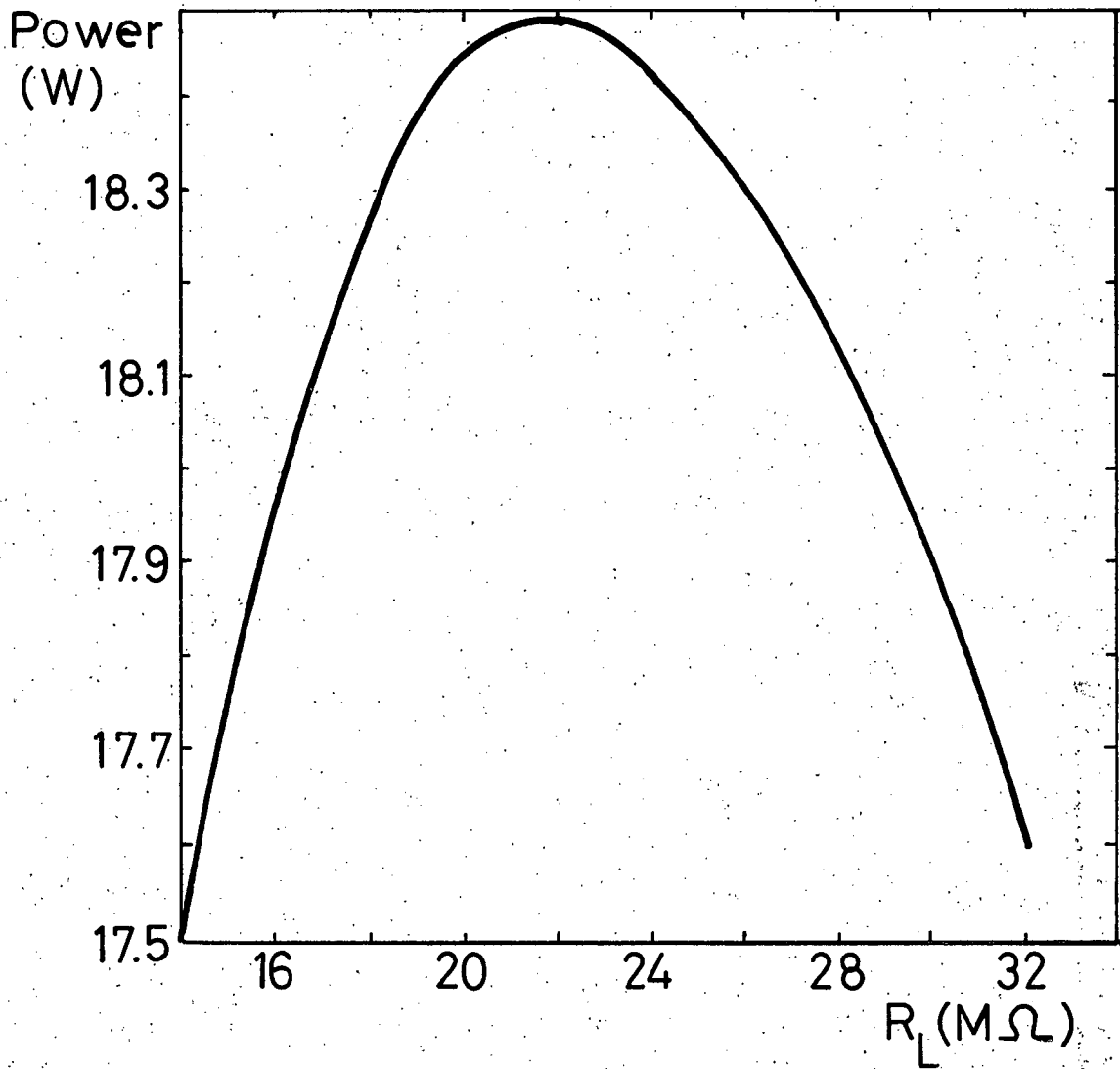


Figure 54 – Power Delivered To a Resistive Load Using Two Semicon Strings

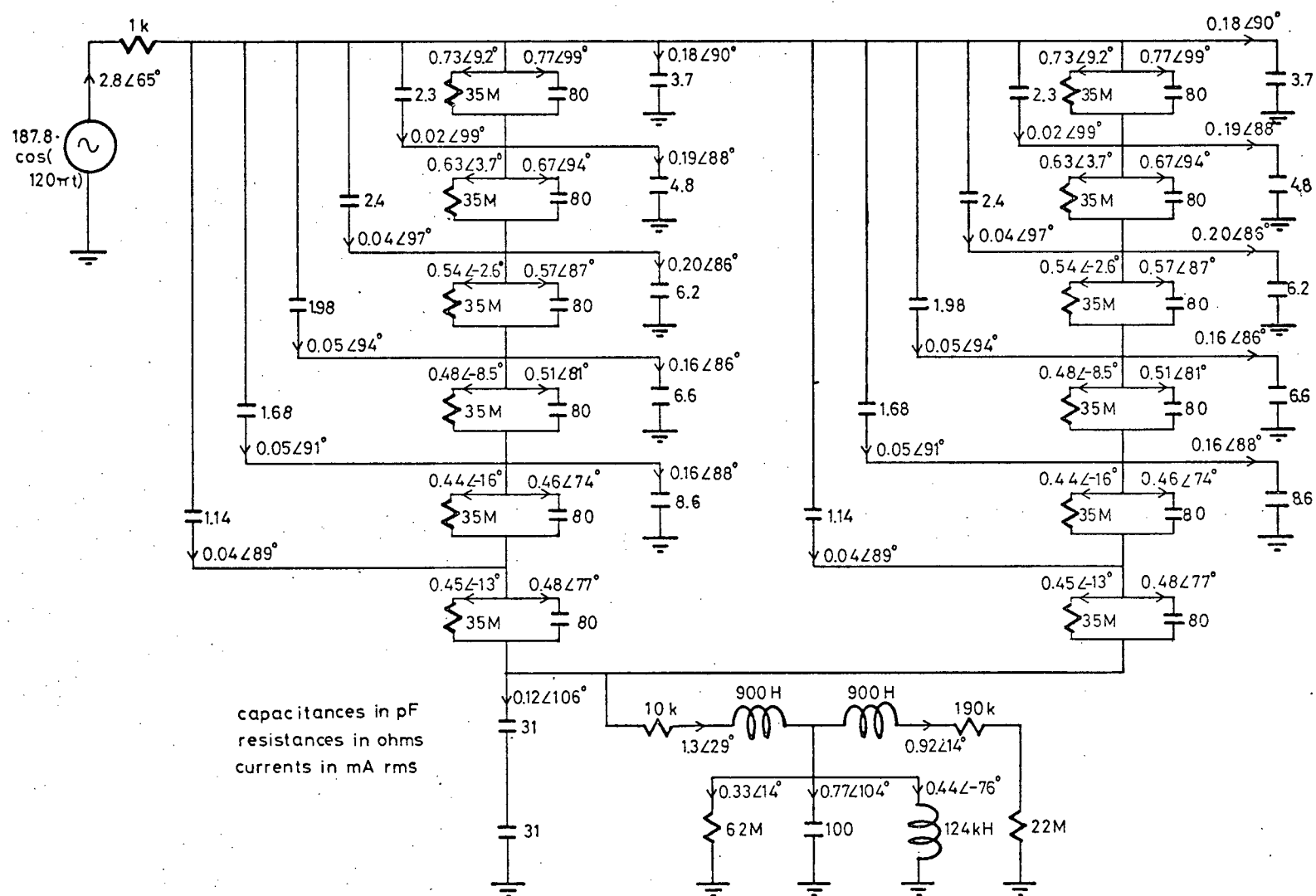


Figure 5.5-Current Distribution For  $R_L = 22 \text{ M}\Omega$

## VI. BEACON POWER SUPPLY AND CONTROL CIRCUITS

### 6.1 Beacon Power Supply Circuit

As mentioned above, the secondary of the transformer can be used to charge either the discharge capacitor of the warning beacon or a high voltage battery pack. A battery pack not only provides standby power in the event of a line outage, but also increases the amount of power which can be extracted from the line. This is because the combination of line and semicon insulator string approximates a constant current source (due to the high impedance of the insulators). Since the average voltage on the discharge capacitor is lower than the voltage of an appropriate battery pack, more power will be delivered to the pack than to the capacitor. For these two reasons only the battery pack power supply will be considered here.

Figure 6.1.1 shows the power supply circuit. A full-wave bridge rectifier is used to charge the battery pack which is made up of 16 12V sealed lead acid ("gel cell") batteries. These batteries have the advantages of standard lead acid batteries without the attendant maintenance problems. Inductor  $L_1$  increases the conduction angle of the rectifier.  $L_2$  is used to tune the magnetizing impedance of the transformer to approximately unity power factor. The zener diodes prevent overcharging of the batteries.

### 6.2 Single Flashtube Control Circuit

Figure 6.2.1 shows the control circuit used with a single flashtube. Programmable unijunction transistor  $Q_1$  is used to form a relaxation

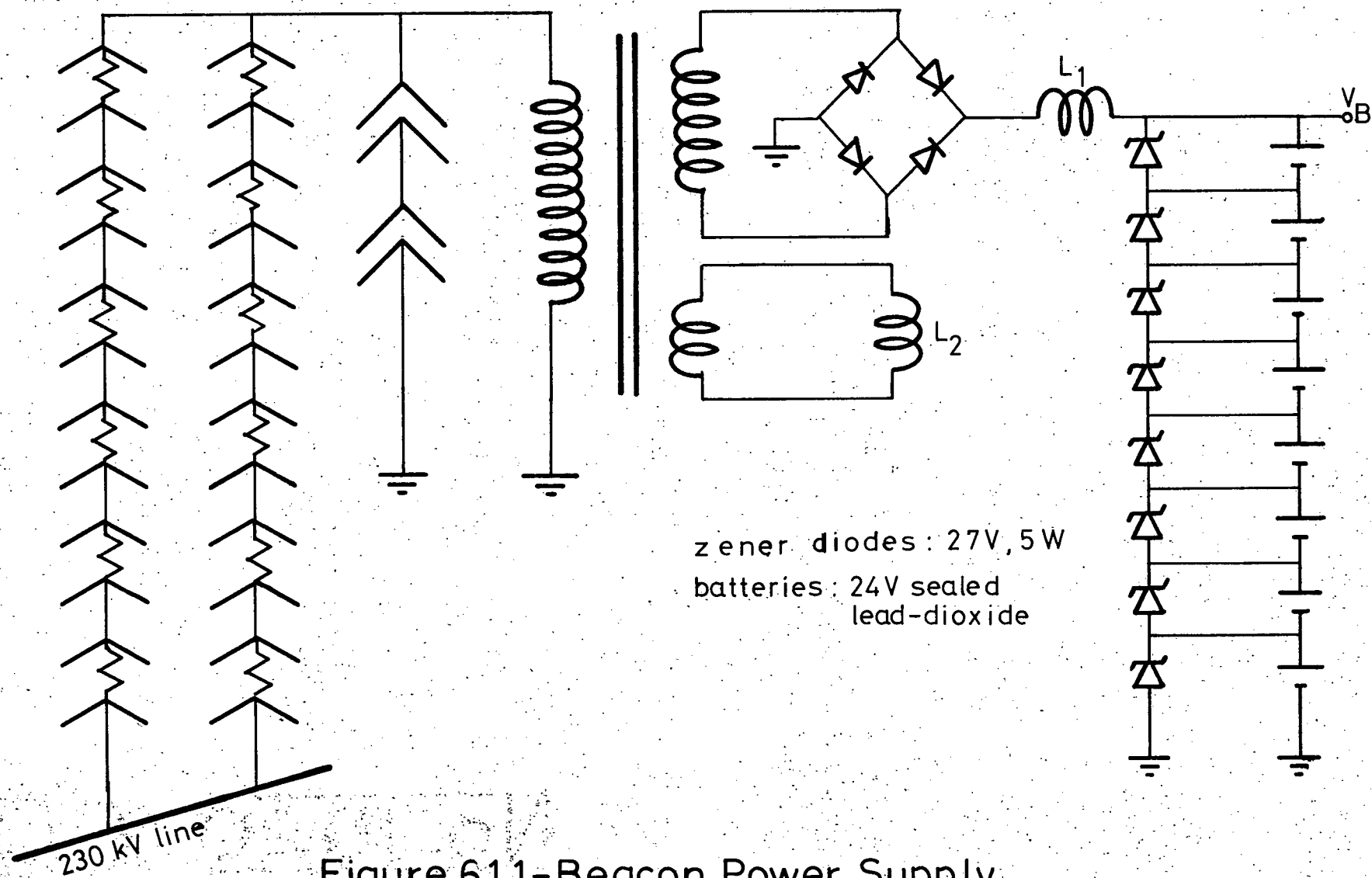


Figure 6.1.1-Beacon Power Supply



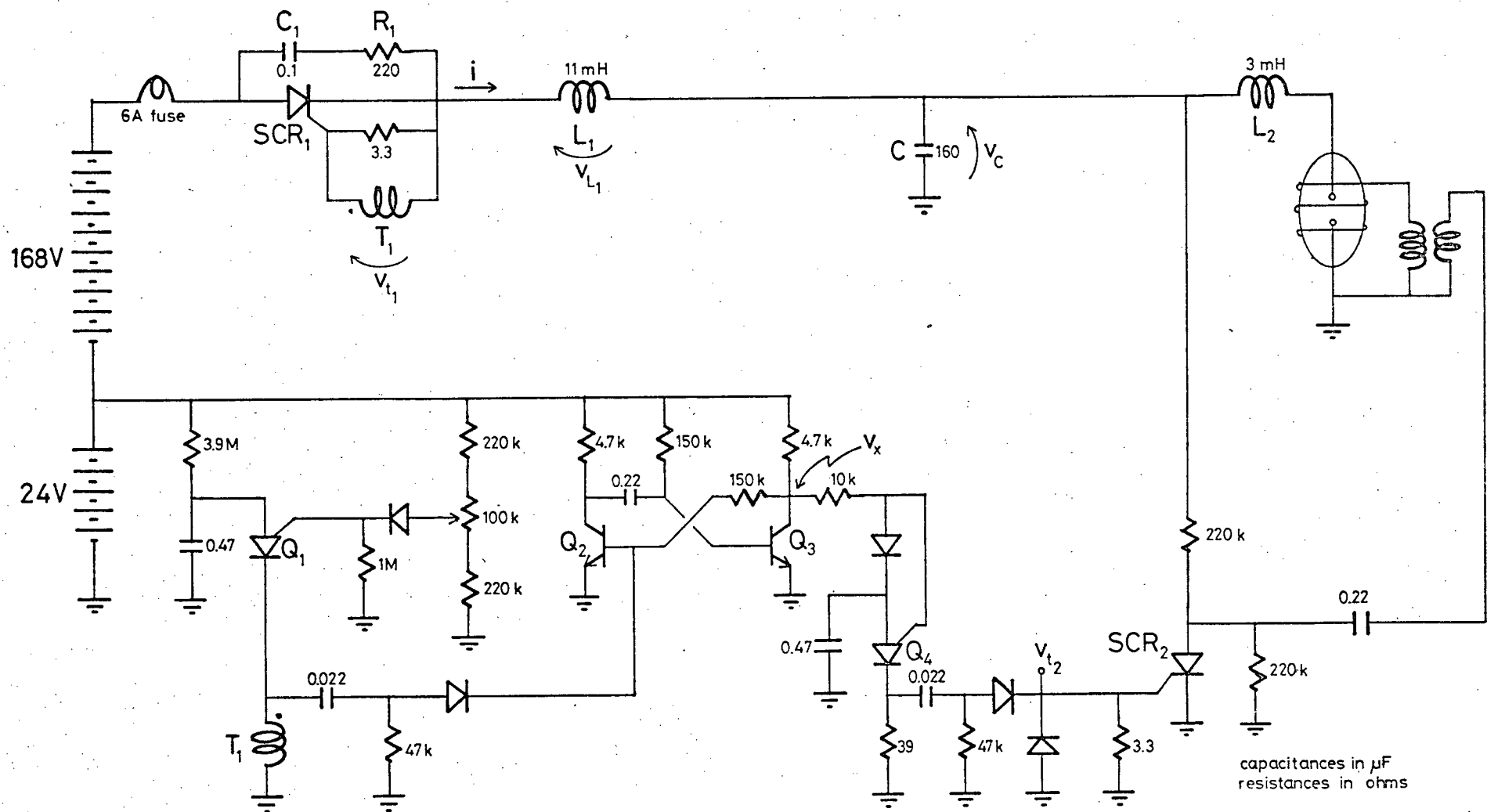


Figure 6.2.1– Single Flashtube Control Circuit

oscillator with a period adjustable around the nominal value of 1 second.

When  $Q_1$  fires,  $SCR_1$  and the monostable ( $Q_2, Q_3$ ) are triggered. Figure 6.2.2 shows the resulting waveforms. When the monostable resets  $Q_4$  fires, triggering  $SCR_2$  which fires the flashtube. It can be shown (Appendix C) that

$$i) \text{ peak current } i_p = \frac{V_B}{\beta L_1} e^{\alpha/\beta \tan^{-1}(-\frac{\beta}{\alpha})}$$

$$ii) \text{ final capacitor voltage } v_{cp} = V_B [e^{\frac{\alpha\pi}{\beta}} + 1]$$

$$iii) \text{ energy delivered by battery } E = C V_B v_{cp}$$

where  $\beta = \sqrt{\frac{1}{L_1 C} - \alpha^2}$ ,  $\alpha = -\frac{R}{2L_1}$ , and  $R$  is the total resistance of the charging circuit (i.e. battery output resistance, series resistances of  $L_1$  and  $C$ ). The energy lost in charging capacitor  $C$  is

$$E_L = E - \frac{1}{2} C v_{cp}^2$$

$$E_L = C v_{cp} [V_B - \frac{1}{2} v_{cp}]$$

This compares favourably with a linear circuit in which the energy lost is  $\frac{1}{2} C v_{cp}^2$  and the final capacitor voltage is  $v_{cp} = V_B$ , requiring a higher voltage battery.

The use of an SCR allows charging the capacitor immediately before the flashtube is triggered, which is advantageous because the capacitors designed for use with flashtubes are quite lossy. The snubber circuit ( $R_1, C_1$ ) prevents triggering of  $SCR_1$  when the flashtube discharges capacitor  $C$ .

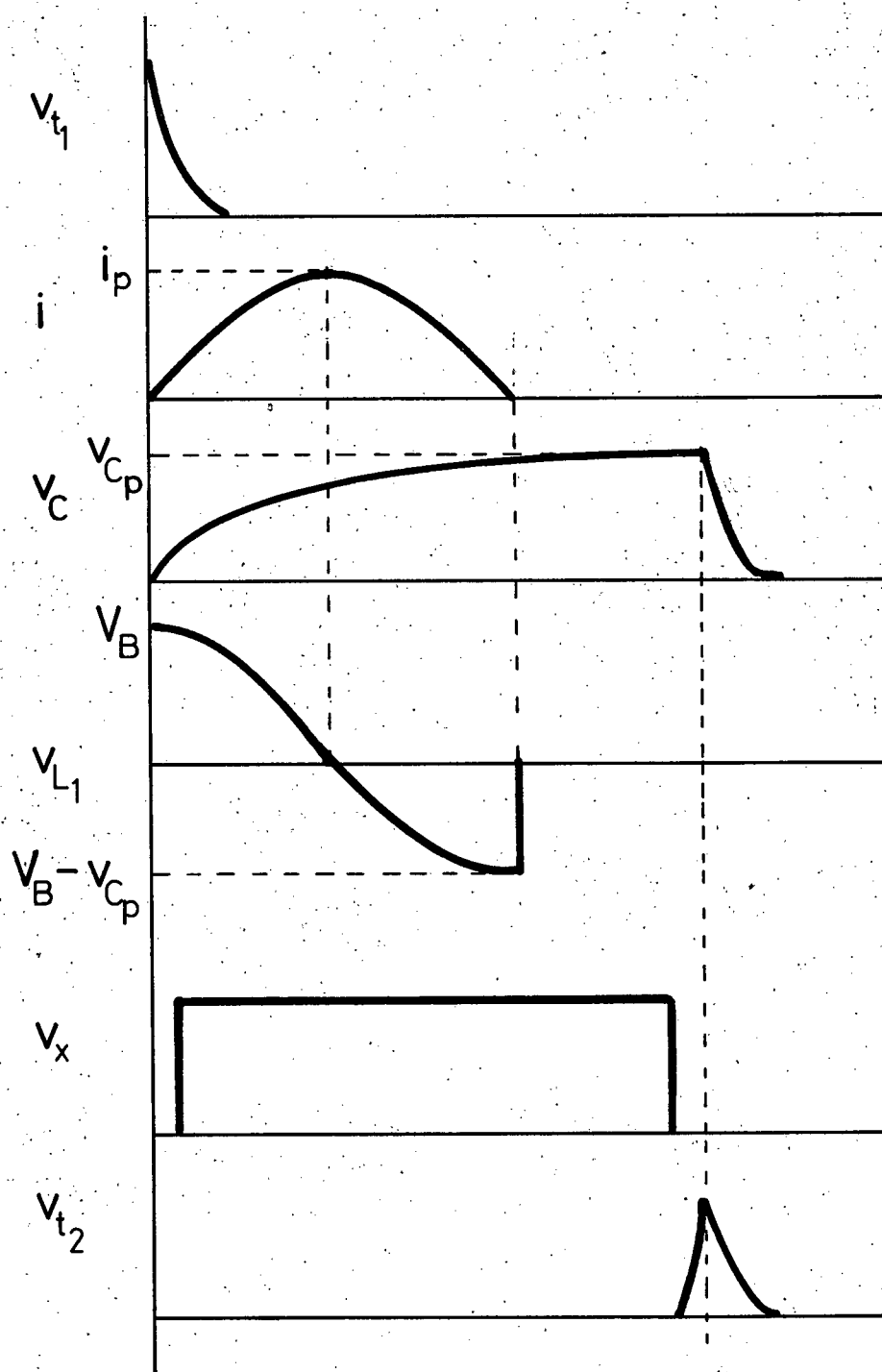


Figure 6.2.2–Waveforms of Control Circuit

### 6.3 Control Circuit for Three Flashtubes

The Ministry of Transport recommendations on warning beacons call for three lights flashing in sequence. Two approaches to extending the single flashtube control circuit to a circuit for three flashtubes are given below. The first has the advantage of redundancy, while the second minimizes the parts count.

Redundancy in a warning beacon system is advantageous when maintenance and monitoring of the system's performance is difficult, as is the case when the beacon is located in a remote area. Three complete single flashtube units, one supplied by each phase of the transmission line, provide maximum redundancy. In the event of a failure in one of the units, or an outage on a single phase of the line, two flashtubes remain operating. To synchronize the three tubes so that they flash in accordance with the MOT regulations, a central control circuit is coupled to the relaxation oscillators of each of the single flashtube control circuits. These relaxation oscillators are set for a period somewhat longer than 1 second, and a trigger signal is capacitively coupled to the gate of the PUT ( $Q_1$  in Figure 6.2). This trigger signal forces the PUT to fire earlier than normal. If the central control circuit fails, each flashtube reverts to single unit operation. Figure 6.3.1 shows the central control circuit.

To minimize the parts count of the beacon system, all three flashtubes can be powered by a single battery pack. The battery pack can be charged by a single transformer fed by six semicon insulator strings in parallel on a single phase, or by three transformers (one on each phase)

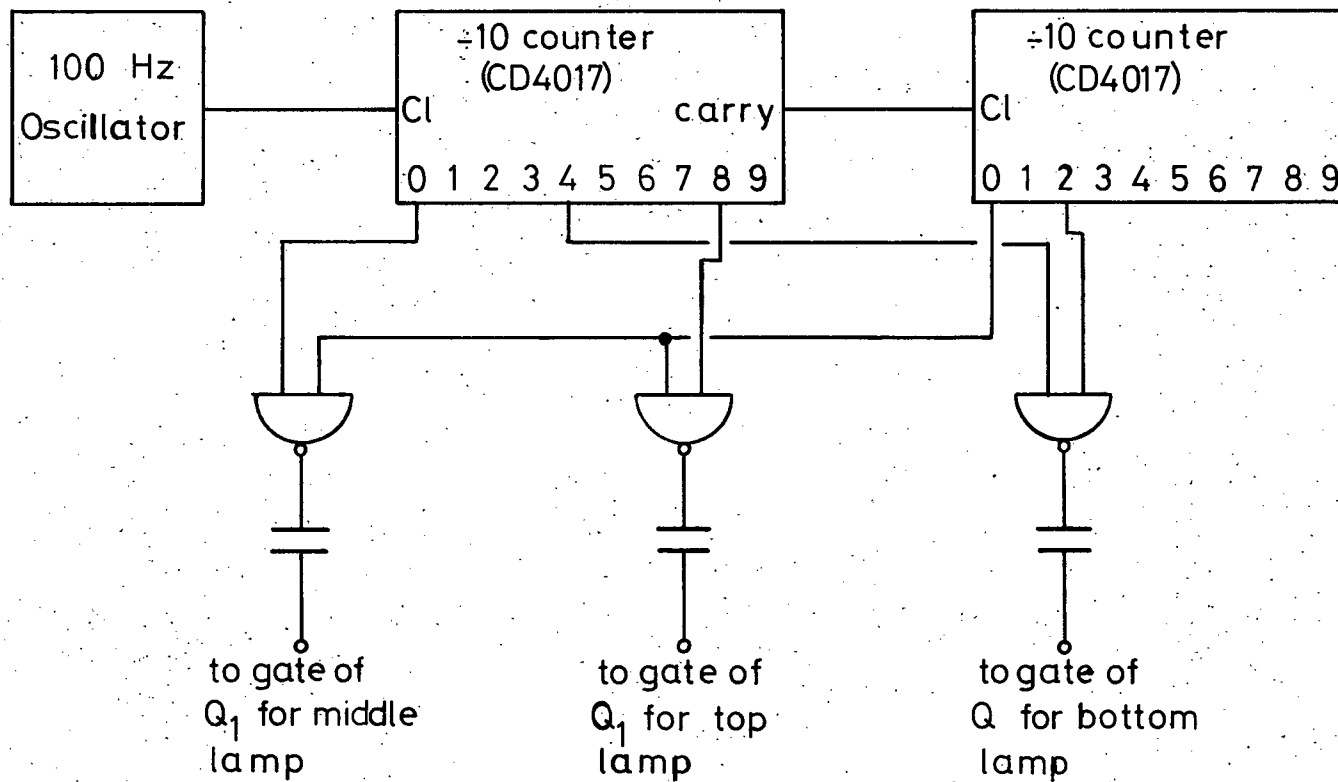


Figure 6.3.1– Synchronizing Signal Generator For Three Single Flashtube Units

and a three phase rectifier. Figure 6.3.2 shows the required control circuit. Its operation is similar to that of the two described above.

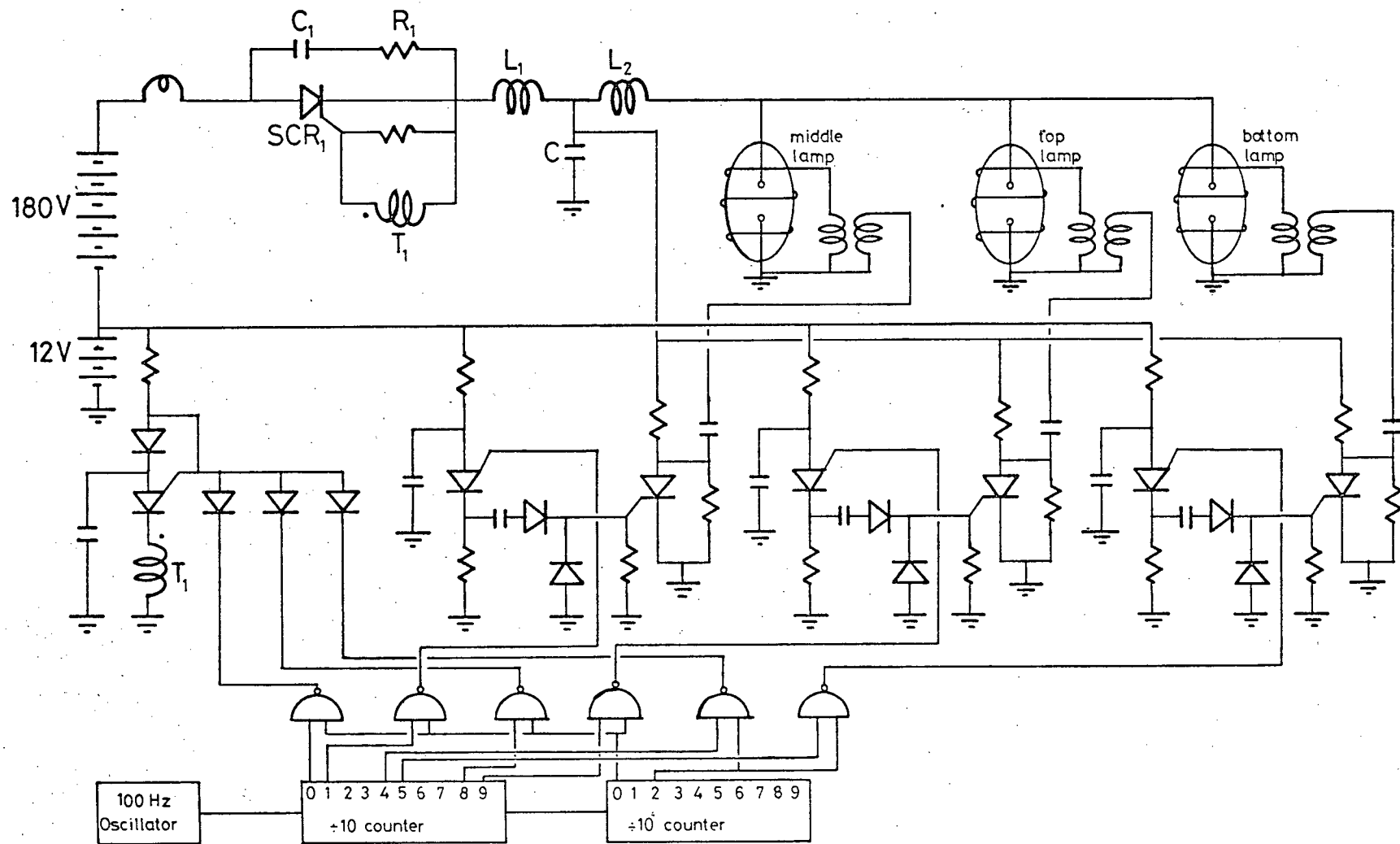


Figure 6.3.2 - Three Lamp Control Circuit

## VII. OBSERVED BEACON PERFORMANCE

A series of tests of a single flashtube warning beacon prototype have been carried out at the Research and Development Laboratory of the British Columbia Hydro and Power Authority. These tests used a step-up transformer providing 80 kV as a power source. This is the line to ground voltage of a 138 kV line. A suitable semicon insulator string for use at this voltage consists of four units. Since the voltage across the primary of the beacon system step-down transformer is approximately equal to the voltage across each unit of the insulator string, the string can be reduced to three units when connected to the transformer without increasing the voltage across the individual units. Alternatively, the full four-unit string may be retained, providing full insulation strength in the event of a transformer failure. Table I summarizes the power available from single and double strings of three and four units. The differences between predicted and observed power for four-unit strings may be explained by the fact that the predictions were made using a higher line voltage and six-unit strings and a resistive load instead of a rectifier and battery load. The prototype beacon consumes 10.2 J of energy per flash, and thus requires two insulator strings in parallel to remain operating.

To observe the charge characteristics of the battery pack in this system, a ten percent charge was established on the batteries, and the system was connected to two four-unit semicon strings in parallel. With the flashtube operating, the batteries were observed to charge over a period of time. Table II and Figure 7.1 show the results.



Table I - Available Power

Semicon Insulator Configuration	Transformer Primary Voltage (kV)	Direct Current Flowing Into A 200V Battery (mA)	Power (W)	Predicted Available Power (W)
1 4-unit string	14	23	4.6	5.8
2 4-unit strings in parallel	22	76	15	18.5
1 3-unit string	-	31.5	6.3	
2 3-unit strings in parallel	25	129	26	

Table II - Battery Charge

Elapsed Time(Hr:Min)	Transformer Primary Voltage (kV)	Charging Current(mA)	Battery Voltage(V)
0:0	20.5	84.5	196.5
22:35	22.6	84.0	208.8
27.50	-	-	209.5
30:10	22.3	82.0	209.1
56:57	23.0	81.8	214
76:30	23.0	82	218
102:00	23.0	80	220
172:40	23.0	79	221
199:10	23.0	79	221
222:00	23.0	79	221

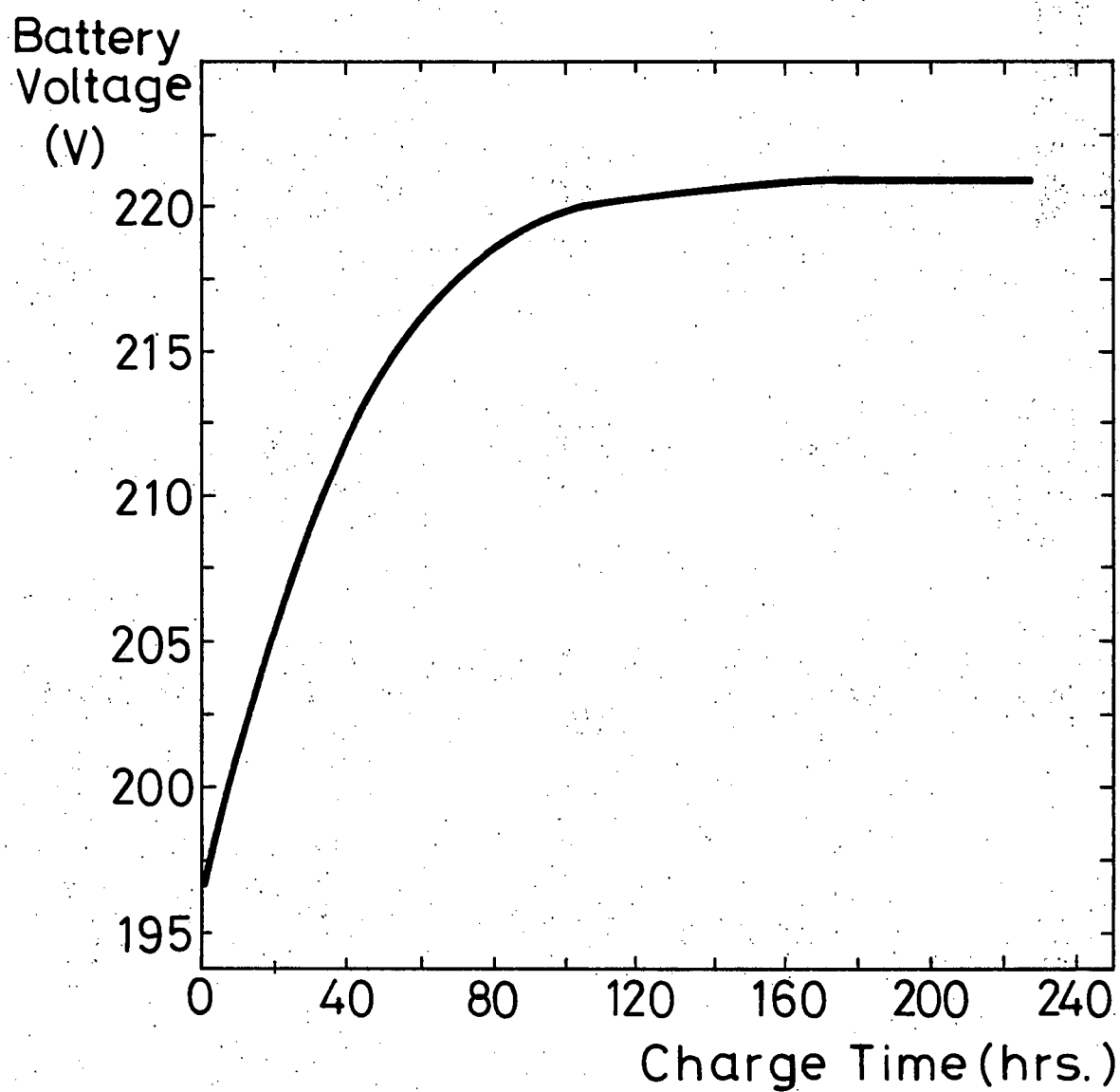


Figure 7.1- Battery Pack Charge Characteristic

### VIII. CONCLUSIONS AND SUGGESTIONS FOR FURTHER WORK

It has been demonstrated that sufficient power can be obtained from the high voltage line through semiconductive glaze insulators to operate a xenon flashtube warning beacon. Whether the light output of the beacon is sufficient to satisfy the Ministry of Transport has yet to be determined.

Performance of the system on a line (as opposed to in the laboratory) needs to be checked. In addition, tests at low temperatures should be carried out, since the leakage current of the insulators will be lower at reduced temperatures. The effectiveness of charging current supplied to the batteries will also be less at lower temperatures.

Consideration should be given to increasing the value of the inductor in series with the battery pack ( $L_1$  in Figure 6.2) to a point where it would prevent discharge of the battery through the flashtube in the event of false triggering. This would increase the reliability of the system.

APPENDIX A - STRAY CAPACITANCE IN THE TRANSFORMER

Let  $C \triangleq$  capacitance/radian from coil to core

$V_c \triangleq$  core voltage

$C_1 \triangleq$  capacitance from core to ground

$C_c \triangleq$  capacitance/radian from coil to ground

$C_t \triangleq$  total interwinding capacitance

$L \triangleq$  inductance/radian<sup>2</sup> of coil

(see Figure A.1)

$$\begin{aligned} \frac{dI}{d\theta} &= \text{difference in current in 2 parts of the coil } d\theta \text{ apart} \\ &= j\omega C(V(\theta) - V_c) + j\omega C_c V(\theta) \end{aligned}$$

$$j\omega C_1 V_0 = \int_0^{2\pi} [j\omega C(V(\theta) - V_0)] d\theta$$

i.e. sum of currents in C flows through  $C_1$

$$\begin{aligned} V_c &= -\frac{C}{C_1} \int_0^{2\pi} (V(\theta) - V_c) d\theta \\ &= \frac{C}{C_1} \left[ \int_0^{2\pi} V(\theta) d\theta - 2\pi V_c \right] \end{aligned}$$

$$\begin{aligned} V_c &= \frac{1}{1 + \frac{2C}{C_1}} \cdot \frac{C}{C_1} \int_0^{2\pi} V(\theta) d\theta \\ &= \frac{C}{C_1 + 2\pi C} \int_0^{2\pi} V(\theta) d\theta \end{aligned}$$

assuming perfect coupling

$$\frac{dV(\theta)}{d\theta} = j\omega L \int_0^{2\pi} I(\theta) d\theta$$

$$\frac{d^2 I}{d\theta^2} = j\omega [C + C_c] \frac{dV(\theta)}{d\theta}$$

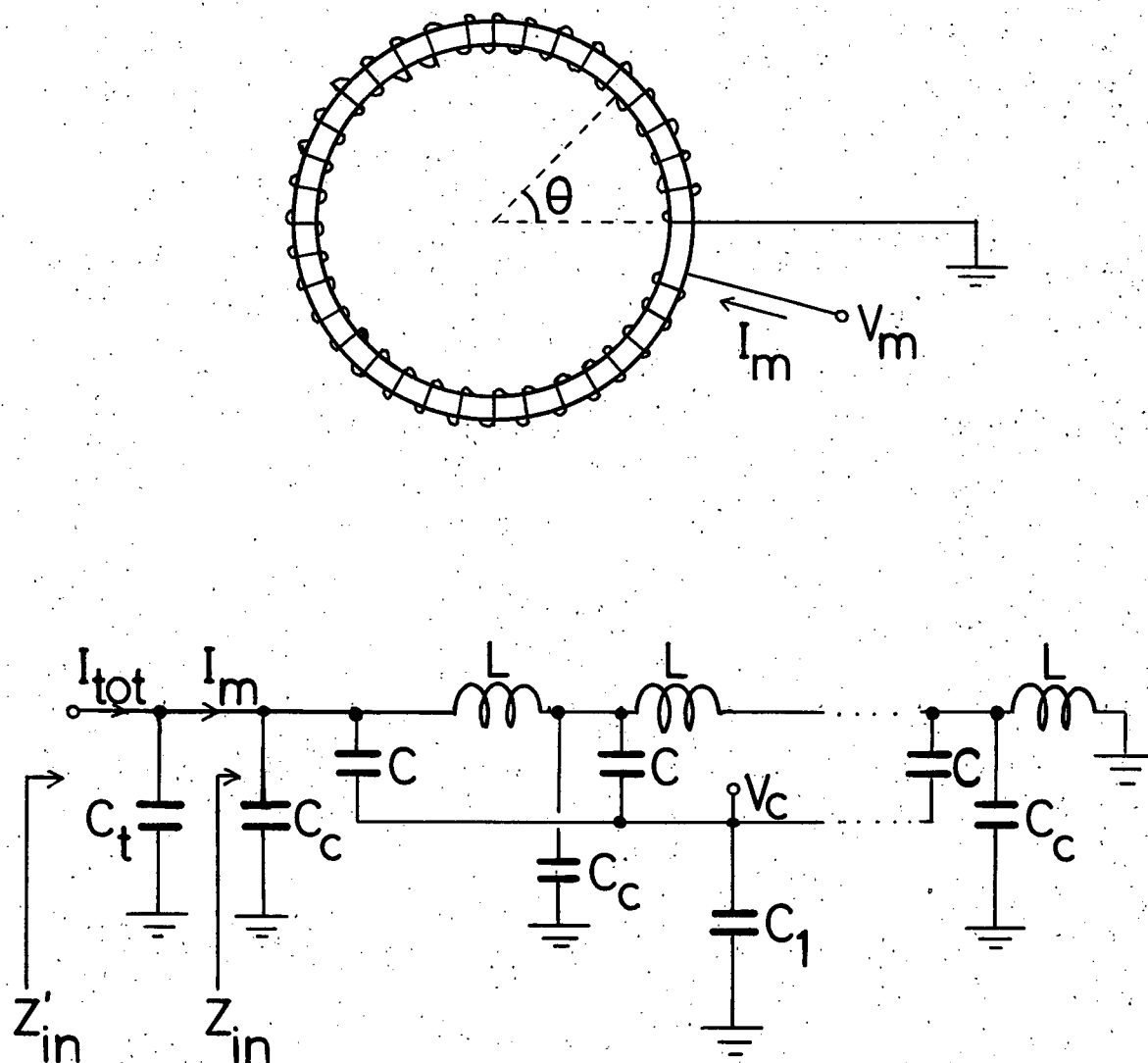


Figure A.1 – Stray Capacitances

$$= -\omega^2 (C + C_0) L \int_0^{2\pi} I(\theta) d\theta$$

$$= -\omega^2 (C + C_c) LA$$

$$\text{where } A \triangleq \int_0^{2\pi} I(\theta) d\theta, \quad \text{a constant}$$

$$\frac{dI}{d\theta} = -\omega^2 L(C + C_c)A\theta + \text{const}$$

$$\left. \frac{dI}{d\theta} \right|_{\theta=0} = -j\omega CV_c + j\omega V(0) (C + C_c)$$

$$\rightarrow \frac{dI}{d\theta} = -\omega^2 L(C+C_c)A\theta - j\omega CV_c$$

$$I(\theta) = -\omega^2 L(C+C_c)A \frac{\theta^2}{2} - j\omega CV_c \theta + B$$

B a constant

$$I(2\pi) = I_m$$

$$\rightarrow B = I_m + \omega^2 L(C + C_c) A \frac{(2\pi)^2}{2} + j\omega CV_c 2\pi$$

$$I(\theta) = I_m + \frac{\omega^2 L(C+C_c)A}{2} [(2\pi)^2 - \theta^2] + j\omega CV_c [2\pi - \theta]$$

$$A = \int_0^{2\pi} I(\theta) d\theta$$

$$\rightarrow A = 2\pi I_m + \frac{\omega^2 L(C+C_c)A \cdot 8\pi^3}{3} + j\omega CV_c 2\pi^2$$

$$A = \frac{2\pi I_m + j\omega CV_c 2\pi^2}{1 - \frac{8}{3} \pi^3 \omega^2 L(C+C_c)}$$

$$I(\theta) = I_m \left[ 1 + \frac{\pi \omega^2 L(C+C_c) (4\pi^2 - \theta^2)}{1 - \frac{8}{3} \pi^3 \omega^2 L(C+C_c)} \right] + j\omega CV_c [2\pi - \theta + \frac{\pi^2 \omega^2 L(C+C_c) (4\pi^2 - \theta^2)}{1 - \frac{8}{3} \pi^3 \omega^2 L(C+C_c)}]$$

$$V(\theta) - j\omega(C+C_c) = \frac{dI(\theta)}{d\theta} + j\omega CV_c$$

$$V(\theta) = \frac{1}{j\omega(C+C_c)} \left[ [-\omega^2 L(C+C_c)\theta] \cdot \frac{2\pi I_m + j\omega C V_c 2\pi^2}{1 - \frac{8}{3}\pi^3 \omega^2 L(C+C_c)} - j\omega C V_c \right] + \frac{C V_c}{C+C_c}$$

$$V(\theta) = - \frac{2\pi\theta\omega^2 LC}{1 - \frac{8}{3}\pi^3 \omega^2 L(C+C_c)} \left[ \frac{I_m}{j\omega C} + \pi V_c \right]$$

$$V_c = \frac{C}{C_1 + 2\pi C} \int_0^{2\pi} V(\theta) d\theta$$

$$V_c = \frac{1}{1 + \frac{4\pi^4 \omega^2 L C^2}{(C_1 + 2\pi C) \left[ 1 - \frac{8}{3}\pi^3 \omega^2 L(C+C_c) \right]}} \left[ - \frac{4\pi^3 \omega^2 L C^2}{(C_1 + 2\pi C) \left[ 1 - \frac{8}{3}\pi^3 \omega^2 L(C+C_c) \right]} \cdot \frac{I_m}{j\omega C} \right]$$

$$V_c = j \frac{4\pi^3 \omega L C I_m}{(C_1 + 2\pi C) \left[ 1 - \frac{8}{3}\pi^3 \omega^2 L(C+C_c) \right] + 4\pi^4 \omega^2 L C^2}$$

$$V(\theta) = j I_m \frac{2\pi\theta\omega^2 LC}{1 - \frac{8}{3}\pi^3 \omega^2 L(C+C_c)} \left[ \frac{1}{\omega C} - \frac{4\pi^4 \omega L C}{(C_1 + 2\pi C) \left[ 1 - \frac{8}{3}\pi^3 \omega^2 L(C+C_c) \right] + 4\pi^4 \omega^2 L C^2} \right]$$

$$Z_{in} = \frac{V(2\pi)}{I_m}$$

$$Z_{in} = j \frac{4\pi^2 \omega^2 L C}{1 - \frac{8}{3}\pi^3 \omega^2 L(C+C_c)} \left[ \frac{(C_1 + 2\pi C) \left[ 1 - \frac{8}{3}\pi^3 \omega^2 L(C+C_c) \right] + 4\pi^4 \omega^2 L C^2 - 4\pi^4 \omega^2 L C^2}{\omega C \left[ (C_1 + 2\pi C) \left[ 1 - \frac{8}{3}\pi^3 \omega^2 L(C+C_c) \right] + 4\pi^4 \omega^2 L C^2 \right]} \right]$$

$$Z_{in} = j \frac{4\pi^2 \omega L (C_1 + 2\pi C)}{(C_1 + 2\pi C) \left[ 1 - \frac{8}{3}\pi^3 \omega^2 L(C+C_c) \right] + 4\pi^4 \omega^2 L C^2}$$

$$L_0 \triangleq 4\pi^2 L$$

$$C_0 \triangleq 2\pi C$$

$$C_2 = 2\pi C_c$$

$$Z_{in} = j \frac{\omega L_0}{1 - \frac{\omega^2 L_0 (C_0 + C_2)}{3} + \frac{\omega^2 L_0 C_0^2}{4(C_1 + C_0)}}$$

$$Z'_{in} = \frac{Z_{in}}{1 + j\omega C_t Z_{in}}$$

$$Z'_{in} = \frac{j\omega L_0}{1 - \omega^2 L_0 \left[ C_t + \frac{C_0 + C_2}{3} - \frac{C_0}{4(1 + \frac{C_1}{C_0})} \right]}$$

so that the effective open circuit input capacitance is

$$C_{eff} = C_t + \frac{C_0 + C_2}{3} - \frac{C_0}{4(1 + \frac{C_1}{C_0})}$$



# APPENDIX B - MAGNETIZING IMPEDANCE OF THE TRANSFORMER

Figure B.1 shows a circuit model of the magnetizing impedance of the transformer.

$$Z_{in} = \left[ \frac{1}{R_m} + j\omega C_{eff} + \frac{1}{j\omega L_m} \right]^{-1}$$

$$= \left[ \frac{j\omega L_m - \omega^2 L_m C_{eff} R_m + R_m}{j\omega L_m R_m} \right]^{-1}$$

$$Z^2 \triangleq |Z_{in}|^2 = \frac{\omega^2 L_m^2 R_m^2}{(R_m - \omega^2 L_m C_{eff} R_m)^2 + \omega^2 L_m^2}$$

$$\omega^2 L_m^2 Z^2 + Z^2 [R_m^2 - 2\omega^2 L_m C_{eff} R_m + \omega^4 L_m^2 C_{eff}^2 R_m^2] = \omega^2 L_m^2 R_m^2$$

$$L_m^2 [\omega^2 Z^2 - \omega^2 R_m^2 + \omega^4 Z^2 C_{eff}^2 R_m^2] - L_m (2\omega^2 C_{eff} R_m Z^2) + Z^2 R_m^2 = 0$$

$$L_m = \frac{2\omega^2 C_{eff} R_m Z^2 \pm \sqrt{4\omega^4 C_{eff}^2 R_m^2 Z^4 - 4Z^2 R_m^2 (\omega^2 Z^2 - \omega^2 R_m^2 + \omega^4 Z^2 C_{eff}^2 R_m^2)}}{2[\omega^2 Z^2 - \omega^2 R_m^2 + \omega^4 Z^2 C_{eff}^2 R_m^2]}$$

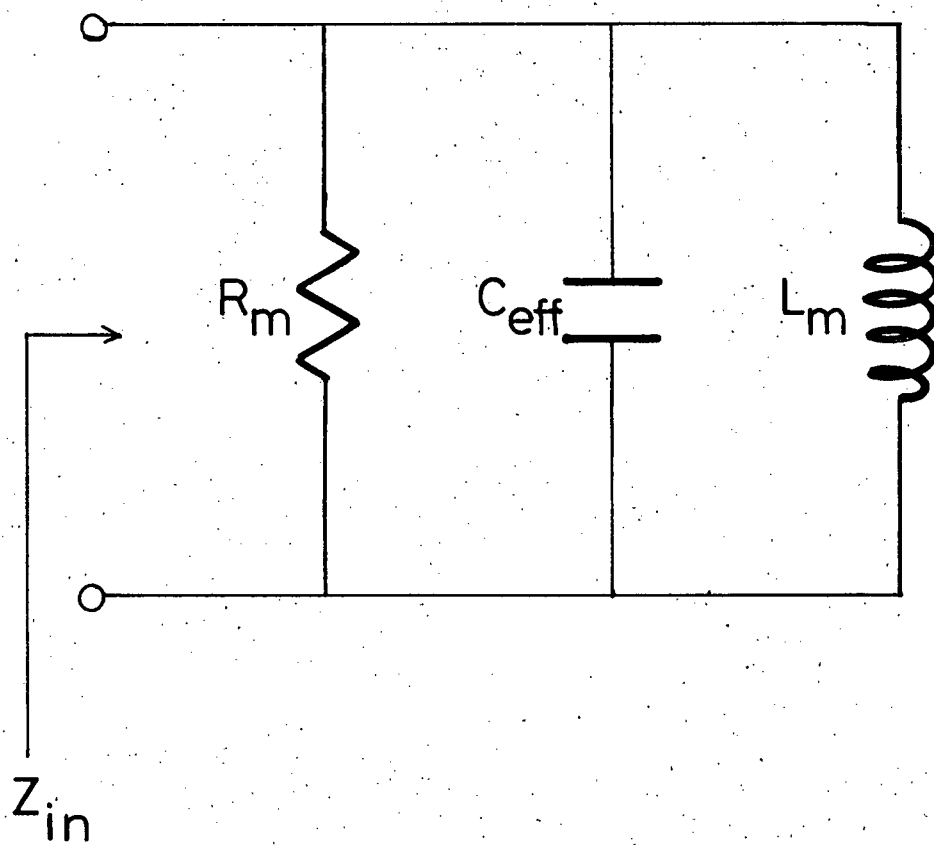


Figure B.1 – Transformer Magnetizing Impedance

### APPENDIX C - CONTROL CIRCUIT WAVEFORMS

The circuit which charges the discharge capacitor may be represented by an underdamped RLC circuit with a step input (see Figure C.1). The differential equation for the current is:

$$\frac{d^2 i}{dt^2} + \frac{R}{L_1} \frac{di}{dt} + \frac{1}{L_1 C} i = 0$$

solving:

$$r^2 + \frac{R}{L_1} r + \frac{1}{L_1 C} = 0$$

$$r = -\frac{R}{2L_1} \pm \sqrt{\left(\frac{R}{2L_1}\right)^2 - \frac{1}{LC}}$$

$$\text{let } \alpha \triangleq -\frac{R}{2L_1}, \beta \triangleq \sqrt{\frac{1}{L_1 C} - \alpha^2}$$

$$\text{then } r = \alpha \pm i\beta$$

$$i = e^{\alpha t} [A \cos \beta t + B \sin \beta t]$$

$$i \Big|_{t=0} = 0 \rightarrow A = 0$$

$$\frac{di}{dt} = \alpha e^{\alpha t} B \sin \beta t + \beta e^{\alpha t} B \cos \beta t$$

$$\frac{di}{dt} \Big|_{t=0} = \frac{V_B}{L_1} = \beta B$$

$$\rightarrow B = \frac{V_B}{\beta L_1}$$

$$i = \frac{V_B}{\beta L_1} e^{\alpha t} \sin \beta t$$

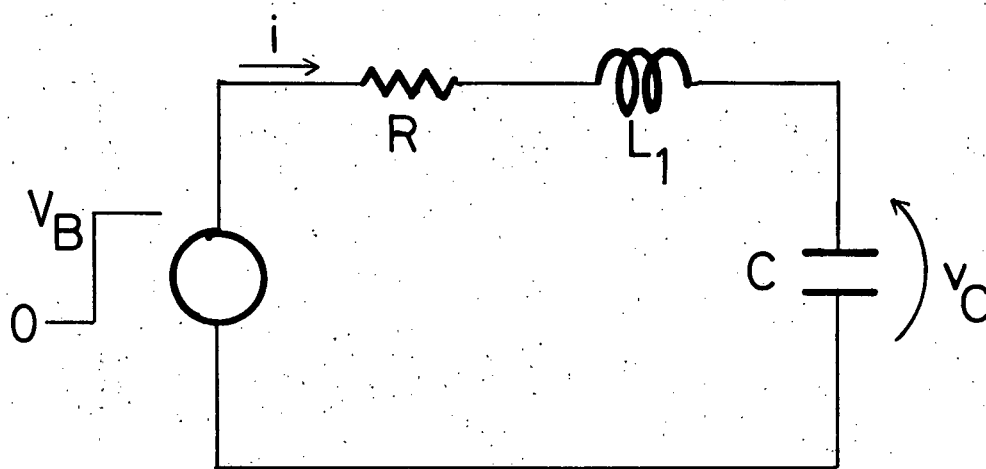


Figure C.1 – Discharge Capacitor  
Charging Circuit

the peak current occurs when  $\frac{di}{dt} = 0$

i.e. when  $e^{\alpha t}(\alpha \sin \beta t + \beta \cos \beta t) = 0$

$$\rightarrow \tan \beta t = -\frac{\beta}{\alpha}$$

$$t = \frac{1}{\beta} \tan^{-1} \left( -\frac{\beta}{\alpha} \right)$$

$$i_p = \frac{V_B}{\beta L_1} e^{-\frac{\beta}{\alpha} \tan^{-1} \left( -\frac{\beta}{\alpha} \right)}$$

at  $t = \frac{\pi}{\beta}$ ,  $i$  becomes negative. In the actual circuit (Figure 6.2) this is prevented by  $SCR_1$ , so that  $i$  remains at zero for  $t \geq \frac{\pi}{\beta}$ .

$$\begin{aligned} v_c &= \frac{1}{C} \int i dt \\ &= \frac{V}{\beta C L_1} \int e^{\alpha t} \sin \beta t dt \end{aligned}$$

$$v_c = \frac{V_B}{\beta C L_1} \left[ \frac{e^{\alpha t}(\alpha \sin \beta t - \beta \cos \beta t)}{\alpha^2 + \beta^2} \right] + \text{const.} \quad [9]$$

at  $t = 0$ ,  $v_c = 0$

$$\rightarrow \text{const.} = \frac{V_B}{(\alpha^2 + \beta^2) C L_1} = V_B$$

$$v_c = V_B \left[ \frac{1}{\beta} e^{\alpha t} (\alpha \sin \beta t - \beta \cos \beta t) + 1 \right]$$

at  $t = \frac{\pi}{\beta}$

$$v_c = v_{cp} = V_B \left[ e^{\frac{\alpha \pi}{\beta}} + 1 \right]$$

the energy delivered by the battery:

$$E = \int_0^{\frac{\alpha \pi}{\beta}} V_B i dt$$

$$\begin{aligned}
 &= \frac{V_B^2}{\beta L_1} \int_0^{\frac{\pi}{\beta}} e^{\alpha t} \sin \beta t dt \\
 &= \frac{V_B^2}{\beta L_1} \left[ \frac{e^{\alpha t} (\alpha \sin \beta t - \beta \cos \beta t)}{\alpha^2 + \beta^2} \right] \bigg|_0^{\frac{\pi}{\beta}} \quad [9]
 \end{aligned}$$

$$= CV_B^2 \left[ e^{\frac{\alpha \pi}{\beta}} + 1 \right]$$

$$= CV v_{cp}$$

REFERENCES

1. Canadian Ministry of Transport, Standards Obstruction Markings, Amendment No. 2 (June 6, 1976), p.22.
2. Dana, Homer J., "An Aviation Hazard Light for Mid-Span Operation on Power Transmission Lines", AIEE Transactions on Power Apparatus and Systems, (December 1960), p. 911.
3. Berthiaume, R.; Blais, R.; D  ry M., Tapping the Overhead Wire on Transmission Lines Produces a 20 kW, 60 Hz Power Supply, Canadian Electrical Association, (March 1977).
4. Berthiaume, R., Study on the Fixed Light Beacon and Its Associate Supply, Canadian Electrical Association, (September 1977).
5. Anglo Corporation, Flashtube Engineering Manual, Anglo Corporation, Rosemont, Illinois, (1974).
6. "IES Guide for Calculating the Effective Intensity of Flashing Lights", Illuminating Engineering, Volume LIX, No. 11 (November 1964), p. 747.
7. Nigol, O.; Reichman, J.; Rosenblatt, G., "Development of New Semiconductive Glaze Insulators", IEEE Transactions on Power Apparatus and Systems, Volume 93 (March/April 1974), p. 614.
8. Rau, N.S., personal communication.
9. Spiegel, M.R., Mathematical Handbook of Formulas and Tables, Schaum's Outline Series, McGraw-Hill (1968), p. 85.